Photorefractive Oscillators

BARUCH FISCHER, SHMUEL STERNKLAR, AND SHIMON WEISS

(*Invited Paper*)

Abstract—**We review recent developments, both theoretical and experimental, involving the nonlinear interactions of light in photorefractive crystals. When pumped by light beams in various configurations, certain crystals, such as barium titanate ($BaTiO_3$), respond with the self-build up of gratings in the crystal and formation of new light beams. The focus of this paper is on these devices, known as photorefractive oscillators, the mutual light-crystal interactions which govern their operation, and all-optical applications which are based on these oscillators.**

The role of optical phases is shown to be prominent in the operation of various photorefractive oscillators. We have developed a theory which accounts for a spontaneous self-frequency detuning of the oscillating beams. This detuning, on the order of 1–10 Hz in $BaTiO_3$, is due to a grating motion in the crystal, which itself is inherently dependent upon the optical phases and amplitudes of the interacting beams in the oscillators and a uniform electric field across the crystal. Experimental evidence points to the presence of an internal electric field in the $BaTiO_3$ crystal which affects the detuning. New experimental results of the detuning dependence on nonreciprocal phases are presented, via the Faraday effect and amplitude aperturing on the oscillating beam. We discuss applications for this new type of dynamic interferometry.

The double phase conjugate mirror (DPCM), a novel oscillator which we have demonstrated, couples mutually incoherent beams in a bidirectional, dynamic holographic link. This new capability significantly relaxes operating requirements, and offers many potential applications in adaptive optics, laser coupling, optical image processing and computing, interferometry, and optical communications. We present new experimental measurements of the transmissivity and reflectivity in the DPCM. Phase-conjugate reflectivity amplification is observed, as predicted by theory. With our invention of the double-color pumped oscillator (DCPO), the DPCM-type configuration is extended to nondegenerate wavelengths. In the DCPO, the two pumping beams are of different colors; nevertheless, a photorefractive oscillation builds up in the crystal. We review the various applications for the DPCM and DCPO, such as beam steering with automatic Bragg matching, image color conversion, and dynamic optical communication interconnects with wavefront matching.

I. Introduction

IN THE past decade, the field of photonics has enjoyed rapid growth. For the transmission of temporal information, fiber optics is already a household word. It is replacing electrical cable in all types of communication networks, from computer communication links to the telephone in the local grocery store. However, the real beauty and power of optics lies in its ability to transmit and process in parallel two- or three-dimensional spatial information. Researchers are investigating different ways of harnessing this vast parallelism in information throughput. Another important goal is the development of nonlinear optical circuitry for various processing tasks. Towards this end, different types of optical logic gates and memories are being investigated. Optical networks are being developed which can mimic some of the fundamental processes which occur in the brain, such as image retrieval by association. Looming over the horizon is the realization of the first optical computer.

In recent years, significant advances have been made in the fields of nonlinear optics and optical computing. The optical computer of the future will rely heavily on nonlinear effects in order to capitalize on the multidimensional parallel processing operations and manipulations that can only be done optically. The realization of fast and efficient real-time spatial light modulation and wavefront color conversion, optical limiting and thresholding, image processing and amplification, beam steering, beam combining, beam cleanup, reconfigurable holographic interconnects and optical memories, and logic gates are some of the challenges in this expanding field of nonlinear optical signal processing. To meet these goals, different materials and physical mechanisms involved in the interaction of light and matter are being studied. These include semiconductors, solid-state (including photorefractive) and liquid crystals, inorganic nonlinear materials, and organic and polymer materials [1].

The past few years have been an exciting and fruitful period for photorefractive (PR) optics, in tune with other significant developments in nonlinear optics. In the high light intensity regime, one of the applications for nonlinear optics is the use of phase conjugate mirrors for aberration correction and coupling of laser systems [2], [3]. For low light intensities, photorefractive materials, first discovered in the late 1960's, are still unique in their ability to display large nonlinearities over the entire visible spectrum, as well as the near infrared. These materials possess an uncanny willingness to display strong nonlinear effects in unique wave mixing configurations. This has led, for example, to the development of various passive phase conjugate mirrors, ring resonators, and beam amplifiers [4]–[11]. Recently, we have developed a new class

Manuscript received March 30, 1988; revised August 23, 1988. This work was supported in part by the Foundation for Research in Electronics, Computers and Communications, administered by the Israel Academy of Science and Humanities, by the National Council for Research and Development, Israel, and by the European Economic Community. The work of S. Sternklar was also supported by a Lady Davis Postdoctural Fellowship at Technion, Haifa, Israel.

The authors are with the Department of Electrical Engineering, Technion—Israel Institute of Technology, Haifa 32000, Israel.

IEEE Log Number 8825896.

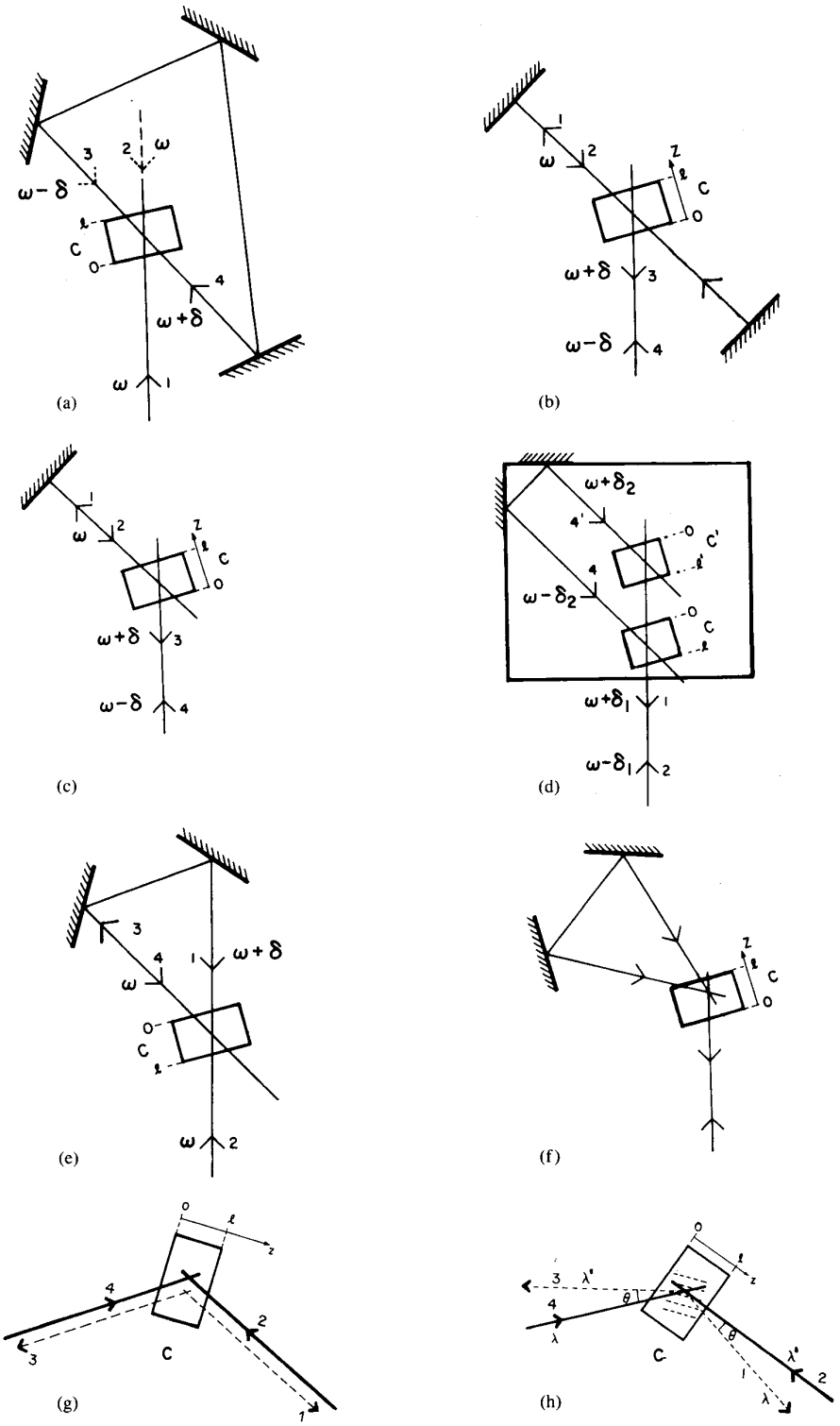

Fig. 1. Photorefractive oscillators. A possible frequency detuning is denoted by δ (as discussed in the text). (a) The bidirectional ring oscillator (with beams 2 and 3 present). The unidirectional ring oscillator (beams 2 and 3 absent). (b) Linear passive phase conjugate mirror (PPCM). (c) Semilinear PPCM. (d) Total internal reflection—TIR (also called two interaction region or "cat") PPCM. The large box is the crystal, with the two interaction regions shown schematically as C and C'. (e) Ring PPCM. (f) A ring oscillator (PPCM) involving six-wave mixing [62]. (g) Double phase conjugate mirror. Input beams 4 and 2 can be mutually incoherent and taken from separate lasers, but are of the same wavelength. (h) Double color-pumped oscillator. Input beams 4 and 2 are of different wavelengths (λ and λ', respectively).

of all-optical image and beam processing applications [12]–[16].

The work reviewed in this paper was done during the period when the emphasis in this field shifted from "phase conjugation" to other real-time optical processing operations, from photorefractive phase conjugate mirrors to photorefractive oscillators, and from an overly simplistic understanding of the wave mixing to a more sophisticated dynamic picture.

The first photorefractive oscillators were demonstrated at the University of Southern California (Feinberg and Hellwarth) [4] and the California Institute of Technology (Cronin-Golomb, Fischer, White and Yariv) [6]–[8], [10]. By externally pumping a $BaTiO_3$ crystal with two counterpropagating beams, a pair of counterpropagating beams built-up as an oscillation between the crystal and an external cavity [4]. Due to the spatially-nonlocal photorefractive response in diffusion dominated crystals, where the grating is shifted with respect to the light interference pattern, the crystal can supply gain to support beams in preferred angular directions. This can be observed in the "fanning effect," which is the result of gratings written by an input beam with deflected portions of itself (scattered noise), resulting in amplification of the scattered beams. In the presence of an external cavity, this "spontaneous" noise can collapse to a stable oscillation state.

Subsequently, a series of photorefractive oscillators were developed [5]–[11]. These various devices are shown in Fig. 1. They include a unidirectional ring oscillator based on two-beam coupling [6], and others based on four-beam coupling. Some of these devices share the ability to self-generate, as an output beam, the phase conjugate of an image-bearing input beam, without the need for external pumping beams. These oscillators are known as self-pumped or passive phase conjugate mirrors (PPCM). The first PPCM's were the linear and semilinear configurations demonstrated at Caltech [6], [7]. Subsequently, the total-internal reflection (TIR, otherwise known as the two-interaction region or "cat" PPCM) [9] and the ring PPCM's [10] were developed. All of these oscillators also included some type of optical feedback to the interaction region, either through external ring or linear paths, or through an internally reflecting loop within the crystal. Since external pumping is not needed, it was obvious to use the passive phase conjugators as end mirrors of a laser resonator, with the ability to oscillate and correct in real time for intracavity phase distortions [7], [11a].

We have recently demonstrated two new photorefractive oscillators: the double phase conjugate mirror (DPCM) [12]–[14] and the double-color pumped oscillator (DCPO) [15], [16]. They are shown in Fig. 1(g) and (h). In these configurations, laser beams from different lasers and even of different colors can mix and "talk" with each other through the nonlinear crystal medium. These beams find each other in a direct bidirectional "handshaking" link, without requiring any optical feedback paths used in the other oscillators. These are significant relaxations of operating conditions, allowing many new applications in adaptive optics and optical processing (e.g., spatial light modulation, filtering and beam cleanup, beam steering, and image color conversion), communications (optical interconnects), interferometry (multimode fiber sensors), and laser coupling and locking. A resonator of two facing DPCM's was shown to support image bearing oscillations [12] with applications in iterative optical processing algorithms (e.g., neural networks and associative memories). We will review these various applications, which present certain solutions to basic problems in electrooptics.

In the following sections of this paper, we will analyze and demonstrate the various temporal and spatial effects associated with photorefractive oscillators. In Section II, we review the development of our theory of self-frequency detuning in these oscillators. Section II-A reviews the developments which led to our present understanding of self-detuning dynamics. Section II-B summarizes our theory of frequency detuning. In Sections II-C–II-E, this theory is applied to the various photorefractive oscillators. Based on these effects, we have suggested the use of the ring PPCM as an optical gyro. This application is described in Section II-F. Interesting detuning effects in the ring PPCM are further described in Sections II-G and II-H. This includes the detuning dependence on magnetic field-induced and aperturing nonreciprocal phases, as well as the effect of an applied electric field. An internal electric field in the crystal is found to effect the detuning dynamics. Section III decribes our recent development of the DPCM and DCPO. In Section III-A, we elucidate the novel processing abilities of these devices which are not shared by other wave mixing configurations. Section III-B reviews the theory of the DPCM. Predictions of reflectivity amplification and symmetrical behavior in this device are verified experimentally. The lack of image crosstalk in the DPCM and other oscillators is treated theoretically in the following section. In Sections III-D and III-E, we review the theory and characteristics of the DCPO, including self-Bragg matched beam steering and image color conversion. A summary of the various envisioned applications for the DPCM and DCPO is given in Section III-F. The paper ends with conclusions in Section IV.

II. Grating Dynamics and Frequency Detuning in Photorefractive Oscillators

A. Background

After the field of real-time volume holography and the basic underlying mechanisms responsible for the photorefractive effect had been established, researchers discovered that by inducing a grating velocity in the crystal, two-wave mixing energy transfer can be enhanced [17], [18]. This was done in crystals such as BSO, which require the application of an external electric field to increase the grating's index modulation ("drift" recording mode), but at the same time resulted in a deviation from $\pi/2$ of the

relative phase between the grating and light intensity pattern. It was understood that a traveling light interference pattern, together with a finite response time for grating formation in the crystal, would contribute a lagging spatial phase shift. This would partially restore the phase shift and lead to greater light energy transfer. This grating motion was induced either by writing the hologram with two coherent beams with a difference in frequency on the order of 10–1000 Hz, or by moving the crystal during the writing process. A similar mechanism is at work in the externally-pumped phase conjugate mirror. A theoretical analysis [5] and experimental measurements [19] of this device reveals that phase conjugate reflectivity is enhanced for nonzero phase shift, and can approach infinity under certain conditions.

In 1984, several groups reported that coupling a TIR PPCM to an untuned dye laser produced substantial line narrowing of the spectrum and generated a slow frequency scanning (~ 5 nm/min) over the laser's gain profile [20]–[22]. This occurred both with a coupled-cavity configuration, as well as when the crystal served as the laser's output mirror. The physical mechanism responsible for this detuning was assumed to be a Doppler frequency shift from moving gratings in the crystal, on the order of 1 Hz for each encounter of the beam and grating. However, the origin of this grating velocity was unclear.

The oscillation frequency in a double phase conjugate resonator (consisting of a cavity bounded by two phase conjugate mirrors) was also found to be slightly detuned [23]. A theoretical anlaysis revealed that a spontaneous grating motion in the crystal supplied the necessary optical phase to fulfill the resonator conditions.

Rajbenbach and Huignard [24] seemed to shed some light on the subject with their report on the operation of the unidirectional ring oscillator using BSO with an applied external field. They postulated that the oscillation was accompanied by a self-induced frequency detuning, in order to enhance the $\pi/2$ grating component, and thus maximize the amplification in the cavity. MacDonald and Feinberg [19] applied the same type of explanation to the self-detuning effects observed in the laser coupled TIR PPCM. They based their theory on the behavior of the externally-pumped phase conjugate mirror with detuned pumping beams. This was also the situation in another theory by Lam [24b].

We have found that the detuning phenomenon in four-wave mixing oscillators is governed by other, more fundamental constraints [25]–[28]. In any configuration in which the grating and light beams build up as an oscillation, amplitude as well as phase conditions must be fulfilled. These constraints do not exist in the externally-pumped phase conjugate mirror, nor in the two-beam coupling amplifier. Thus, conclusions cannot be drawn regarding the behavior of photorefractive oscillators from these devices. We have developed a theory, confirmed experimentally, which accounts for the grating dynamics in four-wave mixing oscillators. The extremely small frequency shifts in slowly responding photorefractive crystals (~ 1–10^3 Hz) might have led to the feeling that they do not have much effect. However, it has been shown to significantly affect the wave mixing in the crystal. The previously-developed model of dynamic four-wave mixing [11] was extended to incorporate the effects of complex beam amplitudes and a uniform electric field in the crystal. This model accounts for many aspects of the dynamic nonlinear interaction between the light beams and the crystal. Using appropriate complex boundary conditions, it predicts the presence of a spontaneous frequency shift in certain photorefractive oscillators, as well as the operation of other novel oscillations [12]–[16]. Our analysis was first applied to the ring PPCM [25], and later to other photorefractive oscillators [27], [28]. A similar approach was taken to explain the dynamics of the two-beam coupling ring oscillator [29], [30] and the linear PPCM [31].

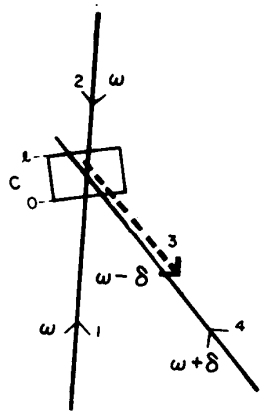

Fig. 2. Four-wave mixing configuration in a photorefractive crystal. With beams 1, 2, and 4 externally supplied, it is an externally-pumped phase conjugate mirror. As in Fig. 1, δ represents a possible frequency detuning.

B. Theory of Self-Frequency Detuning in Photorefractive Oscillators

The configuration of four light beams in the crystal is shown in Fig. 2. These beams are assumed to be plane waves in the xz plane, so that the gratings are of infinite extend along one direction. One may argue that this plane wave picture does not accurately represent reality. A more precise model, for example one incorporating Gaussian beams, would contend with more complex and accurate two- or three-dimensional boundary conditions [32], [33]. In addition, spatially-modulated beams write many sets of gratings with wave vectors along the x and y axes. This plane wave picture, however, is sufficient to satisfactorily account for many dynamic characteristics of photorefractive wave mixing.

A further simplifying situation exists: only one transmission grating builds up due to a dominant electrooptic effect in one preferred direction, and/or the lack of mutual coherency between other potential writing beam pairs. This grating, with wave vector $\vec{k}_g$, is written by beam

pairs {1, 4} and {2, 3} so that

$$\vec{k}_g = \vec{k}_4 - \vec{k}_1 = \vec{k}_2 - \vec{k}_3 \tag{1}$$

where $\vec{k}_i$ is the wave vector of beam i. When other beam pairs are mutually coherent, experimental evidence suggests that other reflection gratings may be superimposed and in some cases cause a lower overall mixing efficiency as well as other changes in a device's characteristics. For phase conjugate mirrors, the phase matching condition of (1) requires that $\vec{k}_4 = -\vec{k}_3$ and $\vec{k}_2 = -\vec{k}_1$. Further on we present a nondegenerate photorefractive oscillator which fulfills (1) without the phase conjugate condition.

Since the photorefractive gratings build up is limited by the time responses of the crystals, the maximum allowed frequency detuning δ between two "writing" beams is bounded and can be neglected in the beams wave equations. (The phase mismatch $\delta l/c \ll 1$, where l is the effective mixing length and c is the speed of light [28].) The detuning is very influential, however, in the photorefractive process itself. This is expressed in the space charge electric field which is induced in the crystal [(3) and (4) below] and in the complex coupling constant (γ in (6) and (7) below). Thus, we can use the degenerate coupled wave equations with the complex coupling constant [25], [28].

The four beams induce the formation of a refractive index grating of the form

$$n = n_0 + \frac{n_g e^{i\phi_g}}{2} \cdot \frac{A_1^* A_4 + A_2 A_3^*}{I_0} \cdot \exp\left[i(\vec{k}_g \cdot \vec{r} - \delta t)\right] + \text{c.c.} \tag{2}$$

where A_i is the amplitude of beam i, $I_0 = \Sigma |A_i|^2$ is the total light intensity in the crystal, n_g is the grating amplitude, ϕ_g is its spatial phase relative to the light intensity pattern, and c.c. stands for the complex conjugate terms. Besides the contributions to the complex grating amplitude via the photorefractive effect, at least three other parameters can change both the amplitude and spatial phase of the grating: a superimposed electric field, nonzero grating velocity, and different wavelengths for the beam couples {1, 4} and {2, 3}. The electric field E_0 can be externally applied or may exist internally in the crystal, such as photovoltaic field. A grating velocity may be externally induced, or may form spontaneously. The effect of different colored beams in photorefractive oscillators is described later on. For the present discussion, we incorporate the effects of E_0 and δ into the wave mixing picture, using the results of the rate equation model of photorefractivity and [11], [28], [33a]

$$n_g e^{i\phi_g} = \frac{-r_{\text{eff}} n_0^3 (\hat{e}_1 \cdot \hat{e}_4^*)}{2} \cdot E_m \tag{3}$$

where

$$E_m = \frac{E_p(E_d - iE_0)}{E_0 + i(E_d + E_p)} \cdot \frac{1}{1 + i\tau\delta}. \tag{4}$$

r_{eff} is the effective electrooptic coefficient, and depends upon the crystal's electrooptic tensor, the beams' polarization, and angular geometry with respect to the crystal's c axis, and other material parameters [11]. n_0 is the ordinary refractive index resulting from the photorefractive effect, and E_{sc} is the space charge field. $E_d = k_B T k_g/e$ and $E_p = e p_d/\epsilon k_g$, where k_B is Boltzmann's constant, T is temperature, ϵ is the dielectric constant, e is the electron charge, and p_d is the trap density in the crystal. τ is the time constant for the grating build up. It is approximately inversely proportional to the total light intensity in the crystal, and is also weakly dependent upon E_0 (this dependence is neglected here). It is the time delay in reacting to the moving grating that introduces the additional spatial phase shift, besides lowering the overall grating amplitude.

Plugging (3) and (4) into the wave equation

$$\nabla^2 E + k^2 E = 0 \tag{5}$$

where $E = \Sigma E_j = \Sigma A_j \exp[i(\vec{k}_j \cdot \vec{r} - \omega t)] + \text{c.c.}$ is the summation of the four waves in the crystal, and invoking the slowly-varying field approximation, results in four coupled-wave equations for the field amplitudes:

$$\frac{dA_1}{dz} = -\frac{\gamma}{I_0} g A_4 \tag{6a}$$

$$\frac{dA_2^*}{dz} = -\frac{\gamma}{I_0} g A_3^* \tag{6b}$$

$$\frac{dA_3}{dz} = \frac{\gamma}{I_0} g A_2 \tag{6c}$$

$$\frac{dA_4^*}{dz} = \frac{\gamma}{I_0} g A_1^*. \tag{6d}$$

$g = A_1 A_4^* + A_2^* A_3$ describes the complex grating structure. γ is the coupling constant which characterizes the strength of the grating, where

$$\gamma = \frac{i\omega n_g e^{i\phi_g}}{c \cos\theta_c} = i\gamma_0 \cdot f(E_0) \cdot \frac{1}{1 + i\tau\delta} \tag{7a}$$

$$f(E_0) = \frac{E_d + E_p}{E_d} \cdot \frac{E_d - iE_0}{E_0 + i(E_d + E_p)} \tag{7b}$$

and

$$\gamma_0 = \gamma(E_0 = \delta = 0) = r_{\text{eff}} n_0^3 \frac{\omega}{2c \cos\alpha_c} \cdot \frac{E_p E_d}{E_p + E_d}. \tag{7c}$$

For simplicity, α_c is taken to be the angle between the normal to the crystal surface and beam 1, as well as beam 4 [11]. In addition, absorption is not accounted for, and is assumed to be negligible. Experimental measurements suggest, however, that this assumption is not accurate.

An exact solution of these coupled-wave equations has been developed [34], by making use of the following con-

servation laws (i.e., quantities that do not vary along the z axis) to decouple (6):

$$A_1A_2 + A_3A_4 = c \tag{8a}$$

$$I_1 + I_4 = d_1 \tag{8b}$$

$$I_2 + I_3 = d_2 \tag{8c}$$

where c, d, and d_2 are constants. Note that $I_0 = d_1 + d_2$ is also conserved. This results in the following algebraic equations:

$$\frac{A_1(z)}{A_2^*(z)} = -\frac{S_-De^{-\mu z} - S_+D^{-1}e^{\mu z}}{2c^*(De^{-\mu z} - D^{-1}e^{\mu z})} \tag{9a}$$

$$\frac{A_3(z)}{A_4^*(z)} = \frac{S_-Ee^{-\mu z} - S_+E^{-1}e^{\mu z}}{2c^*(Ee^{-\mu z} - E^{-1}e^{\mu z})} \tag{9b}$$

where D and E are constants of integration, and with the definitions

$$\Delta = d_2 - d_1 \tag{10a}$$

$$Q = \left(\Delta^2 + 4|c|^2\right)^{1/2} \tag{10b}$$

$$S_\pm = \Delta \pm Q \tag{10c}$$

$$\mu = (\gamma Q)/2I_0. \tag{10d}$$

Applying the boundary conditions of the various two- and four-beam coupling devices, these constants can be found. This will determine their oscillation beam intensities, phase conjugate reflectivity (where applicable), and threshold values of γl, where l is the interaction length in the crystal [11].

By treating the complex amplitudes $A_i(z)$ of the beams in the above model, we have shown that these oscillators exhibit a region of linear dependence of frequency detuning of the oscillating beam on optical phases and/or an electric field across the interaction region [25], [28]. We define the following boundary relations:

$$m_1 \equiv \frac{A_1(0)}{A_2^*(0)} \qquad m_2 \equiv \frac{A_2^*(l)}{A_1(l)}$$

$$r_1 \equiv \frac{A_3(0)}{A_4^*(0)} \qquad r_2 \equiv \frac{1}{m_2}.$$

Referring to the four-wave mixing devices shown in Fig. 1, we see that with the exception of the bidirectional ring oscillator [Fig. 1(a)], all of the devices share the common boundary condition $A_3(l) = 0$. In this case, algebraic manipulations of (8)–(10) result in

$$m_1 = \frac{T + Q}{m_2[(\Delta + B)T + Q]} \tag{11a}$$

$$r_1 = -\frac{(\Delta + 1)T}{m_2[\Delta T + Q]} \tag{11b}$$

where $Q = [\Delta^2 + (\Delta + 1)^2R]^{1/2}$, $T = \tanh[(\gamma l/2)Q]$, $B = (1 + \Delta)R$, $\Delta = [(I_2 + I_3) - (I_1 + I_4)]/I_0$ is the conserved intensity flux (all quantities have been normalized by I_0), and $R = |r_2|^2$ is the reflectivity of the devices at the crystal face $z = l$. The possibility of a frequency detuning and moving grating is incorporated into these relations through T, which depends upon γ [(4) and (7)]. A nonzero detuning renders these equations complex. In the following sections, we will discuss the various photorefractive oscillators and determine their detuning dependence on the beams' optical phases and electric field. Our model predicts that in a linear region of operation this behavior can be simply expressed by

$$\tau\delta = \alpha\theta - \beta E_0. \tag{12}$$

θ is the optical phase associated with an optical feedback path boundary condition, E_0 is a uniform electric field across the crystal, and α and β are material and configurational parameters, respectively.

C. Frequency Detuning in the Ring Passive Phase Conjugate Mirror

The boundary conditions for the ring PPCM, shown in Fig. 1(e), are

$$A_2(z = l) = A_2(l) \tag{13a}$$

$$\frac{A_1(0)}{A_3(0)} = m \qquad \frac{A_4(0)}{A_2(0)} = \tilde{m} \tag{13b}$$

where m and $\tilde{m}$ are the complex amplitude transmissivities of the same optical path for the two counterpropagating beams in the external ring. Thus, $m = \tilde{m}$ unless a nonreciprocal phase of $\theta/2$ exists in the external ring path. In this case, $m\tilde{m}^* = Me^{i\theta}$, where M is the intensity transmittance of the external ring.

As shown in Fig. 1(e), nondegenerate frequencies in this device means that the connected oscillating beams A_3 and A_1 are detuned by δ with respect to the given frequency ω of the inputs A_2 and A_4, accompanied by a grating velocity of δ.

This detuned frequency as well as the reflectivity R of the device can be found by noting that

$$\frac{m_1}{r_1} = m\tilde{m}^* = Me^{i\theta} \tag{14}$$

where θ is any nonreciprocal phase in the ring. Substituting (11) into this relation results in

$$\frac{(T + Q)(\Delta T + Q)}{[(\Delta + B)T + Q](\Delta + 1)T} = -Me^{i\theta}. \tag{15}$$

For the ring PPCM, $\Delta = (1 - M)/(1 + M)$ is known. Equation 15 is the main result, describing the dependence of δ and R on θ and uniform electric field E_0.

Two important characteristics are the $R(\theta)$ and $\delta(\theta)$ behavior. These plots, which display the numerical solution of (15), are shown in Fig. 3 for zero E_0. Around $\theta = 0$ the $\delta(\theta)$ behavior is nearly linear and the reflectivity R is almost constant. The slope and sensitivity are larger for larger M (less loss in the ring) and larger absolute values of $\gamma_0 l$ (greater coupling in the crystal) [25]. The reflectiv-

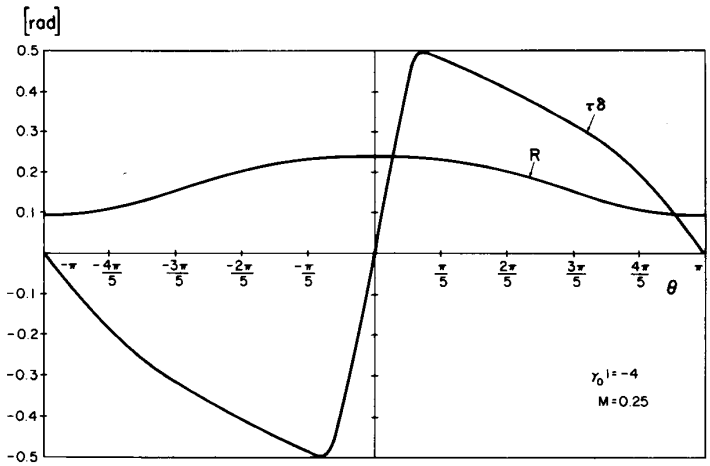

Fig. 3. Theoretical plots of frequency detuning ($\tau\delta$) and reflectivity (R) in the ring PPCM as a function of nonreciprocal phase θ in the external ring, with $\lambda l = -4$ and $M = 0.25$. Around $\theta = 0$, the detuning dependence is nearly linear and R is constant. As explained in the text, the slope of the linear region is tunable via M and γl, and can be shifted along the axis using an applied dc electric field. These characteristics are particularly suitable for an optical gyro.

ity $R \approx M$ in this region. In all of the graphs we observe transition of the slope at the edge of the linear region, characteristic of nonlinear interactions.

An expression for $\tau\delta(\theta, E_0)$ in the linear region can be derived from (15):

$$(\tau\delta) \approx \alpha\theta - \beta E_0 \tag{16}$$

where

$$\alpha = \frac{\sinh \gamma_0 l}{\gamma_0 l} \cdot \frac{M}{M+1}, \quad \beta = \frac{E_p}{E_d(E_d + E_p)}$$

and we approximated $R \approx M$, valid for large $\gamma_0 l$ (for the ring PPCM, $\gamma_0 l$ has a minimum threshold value of 1 at $M = 1$, and increases for lower M), and $E_0 E_p$, $E_0^2 \ll E_d(E_d + E_p)$. For the usual case of $E_p \gg E_d$, the slope of the δ versus E_0 curve is dominated by E_d so that $\beta \approx 1/E_d$.

D. Frequency Detuning in Other Photorefractive Oscillators

We have shown that a self-frequency detuning in the ring PPCM can result from the presence of a nonreciprocal phase. We now turn our attention to the other passive phase conjugate mirrors (PPCM) and ask: does an optical phase dependent detuning exist in these devices?

Referring to Fig. 1, we see that both the semilinear PPCM [Fig. 1(c)] as well as the DPCM (Fig. 1(g), discussed in the next section) have a common boundary condition $A_1(0) = 0$, so that $m_1 = 0$. Recalling (11a), this results in

$$T + Q = 0. \tag{17}$$

Since Q is real, this implies that γ is real for $E_0 = 0$ and thus $\delta = 0$ for any optical phase boundary condition, such as the path between the crystal and external mirror in the semilinear PPCM. In the presence of an electric field, this equation describes the same approximately-linear detuning dependence as in the ring PPCM:

$$\tau\delta = -\frac{E_p E_0}{E_0^2 + E_d(E_d + E_p)} \approx -\beta E_0. \tag{18}$$

Recall the observations of self-scanning in the TIR PPCM. This device may consist of two interaction regions, as shown in Fig. 1(d) [35]. In this figure, it can be described as a ring PPCM with a DPCM in the feedback ring. An analysis [28] of the DPCM shows that it is reciprocal in nature. Using the conservation constant c of (8a), where $c(0) = c(l)$, in conjunction with the boundary conditions of the DPCM $A_3(l) = A_1(0) = 0$, leads to

$$\frac{A_1(l)}{A_4(0)} = \frac{A_3(0)}{A_2(l)}. \tag{19}$$

That is, the counterpropagating beams in the DPCM pick up identical phases. Therefore, the DPCM does not of itself contribute any nonreciprocity to the ring, and, as a result, the TIR PPCM should display similar detuning characteristics as the ring PPCM. We suggest that, as in the ring PPCM, incomplete phase conjugation in the TIR PPCM can be a source of the detuning. The arbitrary sign of the nonreciprocal phase would explain the scanning in both directions. Other experimental evidence, described further on, points to the presence of an internal electric field as a further source of detuning.

A numerical analysis of the frequency detuning in the linear PPCM [Fig. 1(b)] was carried out by Cronin-Golomb and Yariv [31].

E. The Unidirectional Ring Oscillator

The unidirectional ring oscillator, shown in Fig. 1(a), is different from the others in that it is based on two beam coupling. It was theoretically and experimentally shown to exhibit a dependence of frequency detuning on the optical phase in the ring [29], [30], [36]. An exact analytical expression which incorporates both optical phase as well as electric field dependent detuning can be derived by extending the results of [36].

Self-consistency requirements on the phase in the closed loop gives

$$\Delta\phi_{\text{photorefractive}}(E_0, \delta) + \frac{\omega L}{c} = 2\pi s \tag{20}$$

where s is an integer, L is the ring length (including the effective light path in the photorefractive crystal), and $\Delta\phi_{\text{photorefractive}}$ is the additional phase picked up in the crystal by the circulating beam due to the nonlinear wave mixing [36].

$$\Delta\phi_{\text{photorefractive}} = -\ln M \quad \frac{2\ \text{Im}\ (\gamma)}{\text{Re}\ (\gamma)} \tag{21}$$

where M is the intensity transmissivity in one complete round-trip in the ring. We also define the effective phase of the passive ring as $\theta = \omega L/c - 2\pi s$, where θ is the interval $(-\pi, \pi)$. Using (7), (20), and (21), we obtain

$$\tau\delta = \frac{\dfrac{-2}{\ln M}\theta - \dfrac{E_p}{E_0^2 + E_d(E_d + E_p)}E_0}{1 + \dfrac{2}{\ln M}\dfrac{E_p}{E_0^2 + E_d(E_d + E_p)}\theta\, E_0}. \tag{22}$$

For a small electric field such that $E_0^2 << E_d(E_d + E_p)$, this reduces to

$$\tau\delta \approx \frac{\alpha'\theta - \beta E_0}{1 + \alpha'\beta\theta E_0} \tag{23}$$

where $\alpha' = -2/\ln M$, and, as in the ring PPCM, $\beta = E_p/E_d(E_d + E_p)$. For $\alpha'\beta\theta E_0 << 1$, (23) reduces to an approximate linear dependence:

$$\tau\delta \approx \alpha'\theta - \beta E_0. \tag{24}$$

F. The Ring PPCM as a Gyroscope

Our theory suggests that the ring PPCM can be used as an optical gyroscope [25]. A nonreciprocal phase exists in the ring if the device is rotating, and is translated into a measurable frequency detuning. This new type of "active" interferometry can also incorporate a multimode fiber in the ring, since the counterpropagating beams in the ring are a phase conjugate pair, and thus cancel out the modal dispersion of the fiber. We stress that in this device the dynamic photorefractive wave mixing converts phases into a frequency detuning. This is fundamentally different from other phase conjugate gyros [37], [38].

Using this device as an optical gyroscope for different regimes of rotation rates depends on the crystal time constant τ and the total ring area (diameter and total length). Significant nonreciprocal phase shifts due to rotation may be obtained by long fibers as in fiber gyros. The θ dependence on the rotation rate Ω for a ring consisting of a coil of fibers of total length L and ring diameter D is given by [39]

$$\theta = (2\pi LD/\lambda c)\Omega \tag{25}$$

where λ and c are the wavelength and velocity of light in vacuum. Thus we obtain for the ring PPCM

$$\delta = \frac{\alpha}{\tau}\left(\frac{2\pi LD}{\lambda c}\right)\Omega. \tag{26}$$

For long fiber lengths, even a small frequency difference between the counterpropagating beams in the ring will cause another nonreciprocal phase term $\theta' = L\delta n/c$, where n is the ring's index of refraction. Substituting

$$\theta \rightarrow \theta + \theta' = \theta + [Ln/\tau c](\tau\delta) \tag{27}$$

into (15) results in an enhancement of the detuning in the linear region [25].

We have pointed out that an electric field can be used to bias the operating point of the gyroscope. The transmissivity M through the ring can be another controlling parameter [26].

G. Frequency Detuning via Faraday and Amplitude Aperturing Loss Nonreciprocities in the Ring PPCM

We have shown that a nonreciprocal phase source in the ring PPCM will cause a frequency detuning. Rotating the ring will cause such a condition through the Sagnac effect. The Faraday effect is also nonreciprocal in nature. We have reported that this effect induces a detuning [25]. Recently, a detailed demonstration has been given [40] which confirms this picture.

The experimental configuration is shown in Fig. 4. The 514.5 nm line of the argon ion laser was guided into the $BaTiO_3$ crystal as shown to form a ring PPCM. A multimode fiber was held within a solenoid and placed in the ring path as shown (the knife-edge K was not used for this experiment). The fiber was a multimode preform fabricated from Hoya FR-5 paramagnetic glass [41]. The outer and core diameters were 1.8 and 0.4 mm, respectively, with a length of 15 cm. The length of the solenoid was 12.5 cm, and generated a magnetic field B of 480 G at 1 A. We measured a Verdet constant V of 5.79×10^{-5} rad/G · cm for the fiber, which gives a polarization rotation $\phi = V \cdot B \cdot d$ in the solenoid of length d. The nonreciprocal phase in the ring is $\theta = 2\phi$ for any component of the polarization. With linearly polarized light entering the fiber, we measured a polarization ellipticity of less than 0.1 at the fiber output, indicating small birefringence or intermodal polarization scrambling for this fiber. The fiber's intensity transmissivity was 0.8. All of these measurements were done at $\lambda = 514.5$ nm.

Varying the dc current to the solenoid changed the frequency detuning of the oscillating beam. A sample plot of this detuning in output beam 1 (measured interferometrically with respect to input beam 2), is shown in Fig.

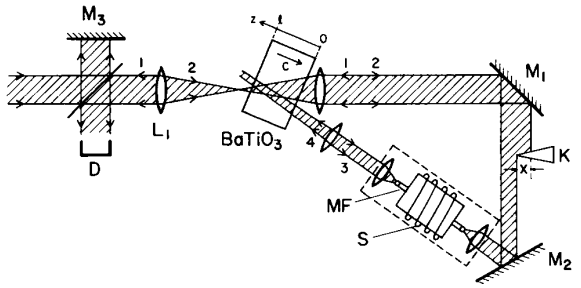

Fig. 4. Experimental schematic incorporating Faraday and amplitude aperturing loss nonreciprocities in the ring PPCM. In the Faraday experiment, the knife-edge K was not present. In the knife-edge experiment, the elements in the dashed box were removed. MF: multimode Faraday fiber, S: solenoid, D: detector to measure frequency detuning of output beam 1.

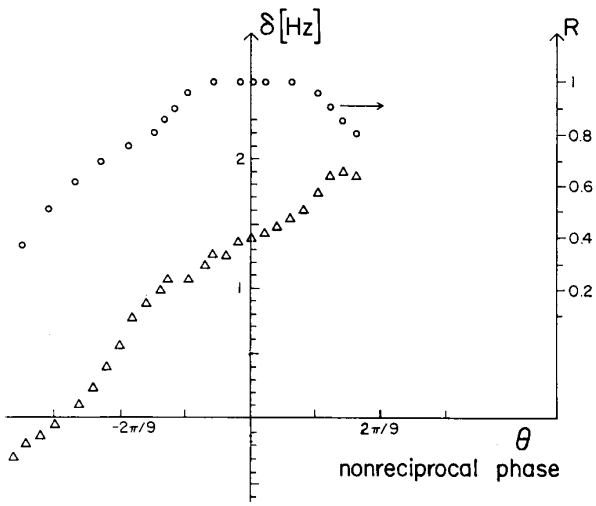

Fig. 5. Sample plots of measured detuning (triangles) and normalized (the maximum 1) reflectivity (circles) in the ring PPCM versus applied nonreciprocal phase θ via the Faraday rotator.

5. Included is a plot of the measured reflectivity. Maximum reflectivity was recorded for zero applied nonreciprocal phase (i.e., zero magnetic field) and decreased for increasing magnetic field. Theory predicts, however, maximum reflectivity for zero frequency detuning and decreasing reflectivity for increased detuning. This experimental behavior results from the lower coupling of beams 1 and 4 to the wave mixing due to the polarization vector rotating away (via the Faraday effect) from the optimum extraordinary polarization state. This also causes a decrease in the mixing efficiency due to the ordinary polarization component. In an experiment by Jiang and Feinberg [40] using a Faraday rod, this polarization artifact was eliminated.

One of the basic differences between the ring PPCM and other PPCM's such as the semilinear PPCM, is that the oscillation builds up in one direction (clockwise as beams 1 and 3 in Fig. 4) while beam 2 is supplied externally. If these counterpropagating beams have different optical paths, they introduce nonequal optical lengths and phases, and should result in a detuning. This condition will occur, for example, if a spatial amplitude modulation is inserted in the ring cavity, as shown in Fig. 4. In the upper part of the ring (between the crystal C and the blocking element K) the counterpropagating beams differ in their spatial structure and phase fronts (by virtue of the spatially-dependent absorption and subsequent diffraction), and will thus deviate from being a phase conjugate pair of beams. The 2D amplitude modulation thus introduces an effective nonreciprocal phase, besides reducing the overall transmissivity of the ring and a possible deterioration of the phase conjugation quality of the reflected beam 1. In an experiment, described below, we introduce this spatial modulation by sliding a knife-edge through the ring oscillation.

The length of the external ring path was 144 cm. The fiber and solenoid were removed. A knife-edge K was placed midway around the ring, between mirrors M_1 and M_2, where it was moved into the beams' path from the outside using a micrometer. The detuning of output beam 1 for a sample run, measured interferometrically, is shown in Fig. 6 for varying knife-edge position. The spot size of beam 2 (which was approximately collimated between the lenses in the ring) at the knife was about 1.3 mm. The oridinate units are normalized knife position along the beam, i.e., 0.1 denotes 10 percent of beam 2's spot diameter blocked. The observed detuning behavior was repeatable for this knife-edge position.

The presence of the knife-edge in the cavity dictates that beams 1 and 4 will have different spatial mode patterns, beam curvatures, and slightly different paths, which leads to an average nonequal (nonreciprocal) phase. Assuming that the counterpropagating beams in the lower half of the ring in Fig. 4 (beams 3 and 4 between the crystal and the knife-edge) are nearly a phase conjugate pair, then the significant phase nonreciprocity enters in the upper half of the ring, between beams 1 and 2. These beams have slightly different optical paths in this portion of the ring and different widths. For example, the formula for the Gaussian waist (ω_0) dependent phase [42] $\eta(z) = \tan^{-1}(\lambda z/\pi w_0^2 n)$ shows a phase difference of 0.32 rad between these beams, assuming a waist of 1 mm for input beam 2 and 0.5 mm for oscillation beam 1 due to the blocking, a path length $z = 70$ cm between the crystal and knife edge in the upper half of the ring, $\lambda = 514.5$ nm, and $n = 1$. The detuning curve displays a strong dependence upon the knife position and appears to approach one period for x approaching 1. The oscillation decays however, for significant blocking in the ring, as seen in the accompanying phase conjugate reflectivity curve.

Other researchers have reported that varying the input beam curvature to a TIR PPCM serving as one end mirror to a dye laser [22], or rotating one of the external mirrors in a ring PPCM coupled to a semiconductor laser [43], so that the ring is misaligned, leads to a change in the frequency scanning direction. Those effects may be connected to the aperture-dependent detuning described here. A recent experimental study showed a nice interplay be-

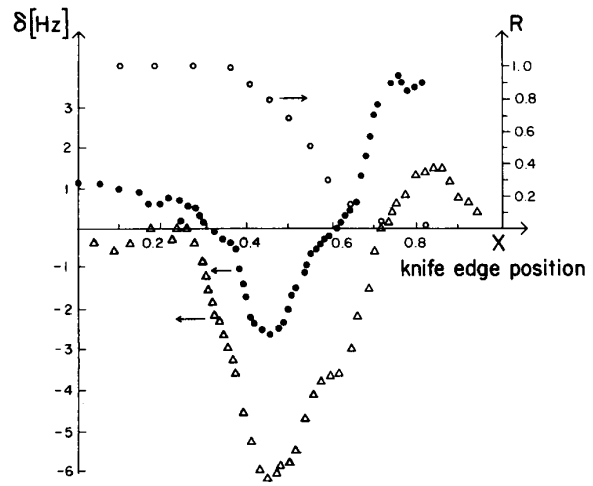

Fig. 6. Sample plots of measured detuning and normalized reflectivity in the ring PPCM versus knife-edge position across the beam profile in the ring.

tween the two different nonreciprocal phase sources: Faraday and nonreciprocal transverse modes [40]. This is in line with our present understanding of the detuning dynamics.

H. Electric Field-Dependent in Photorefractive Oscillators

We have experimentally studied two different four-wave mixing configurations: the semilinear PPCM and the ring PPCM [27]. The ring and semilinear configurations differ fundamentally in their detuning characteristics, as can be seen from (16) and (18). The semilinear PPCM has a wide region of an approximately linear detuning dependence of a dc electric field along the grating wavevector, but is independent of any optical phase conditions in the photorefractive cavity. Therefore, for $E_0 = 0$, $\delta = 0$ as well, and the oscillation is degenerate.

In a semilinear PPCM, an applied electric field E_A was regulated by a dc voltage supply source [27]. Extraordinarily polarized light from the 488 nm line of an argon ion laser without an etalon was focused with a beam spot diameter of approximately 1 mm in the crystal. The detuning was measured interferometrically as shown.

A sample of typical plots of the measured detuning dependence on an electric field are shown in Fig. 7, for slightly-varying crystal orientation or input power density. Here δ is the frequency detuning of beams 1 and 3 from beams 4 and 2, respectively, or half the detuning of output beam 3 with respect to input beam 4. The intensity of the oscillation did not change appreciably for different E_A, thus I_0 was approximately constant. Invariably, we observed small positive detuning for a zero applied field which decreased to zero in the region $E_A \sim 0.2$ kV/cm. These graphs indicate that an internal electric field $\vec{E}_{IN}$ exists within the crystal. This field may be due to the bulk photovoltaic effect which causes an electric field to form along the c axis (or z coordinate). From the angular con-

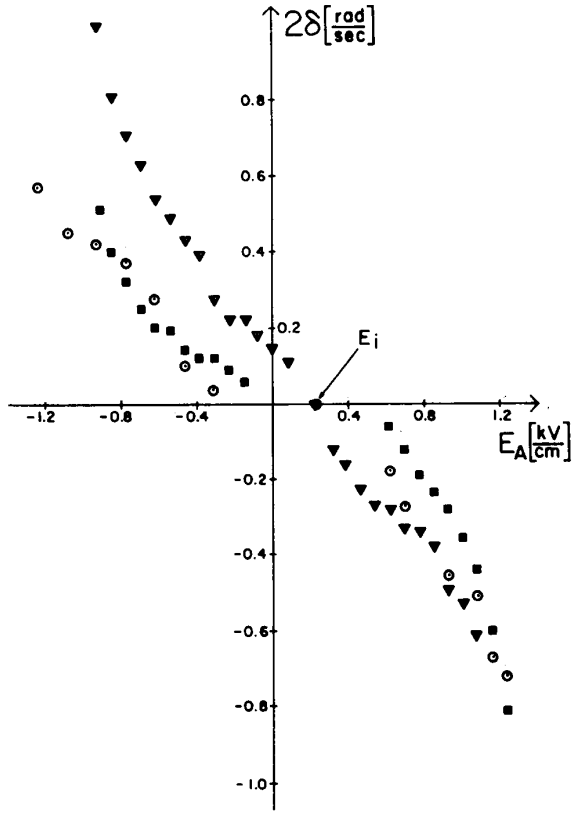

Fig. 7. Measured detuning in the semilinear PPCM versus applied dc field. In all the runs, detuning went to zero at $E_A = E_i \approx 0.2$ kV/cm, indicating the presence of an internal field in the crystal.

figuration, we estimate the value of this field along the c axis to be about 0.7 kV/cm. The actual electric field may be different due to inhomogeneous voltage drops between the electrodes and crystal or within the crystal itself. Other researchers have also recently reported the presence of an internal field in $BaTiO_3$ [44], [45]. The existence of internal fields in this crystal, its source, as well as its magnitude, have been points of controversy for some time [3], [19], [46], [47].

Turning to the ring PPCM, we measured $\delta(E_A)$ for this device [27]. Typical plots are shown in Fig. 8 for slightly varying crystal or external ring orientations. The difference between these plots and those of the semilinear PPCM is due to the $\alpha\theta$ term in the detuning expression for the ring PPCM [(16)]. As was discussed previously, a nonreciprocal phase θ may be due to incomplete phase conjugation which would result in different complex amplitude transmissivities for the counterpropagating beams in the ring.

To summarize: the observed electric field and optical phase dependent detuning corroborates our theory of frequency detuning in these oscillators. The linear dependence of the detuning on an electric field, which we have experimentally verified, contrasts with a predicted inverse dependence of a different theoretical model [24].

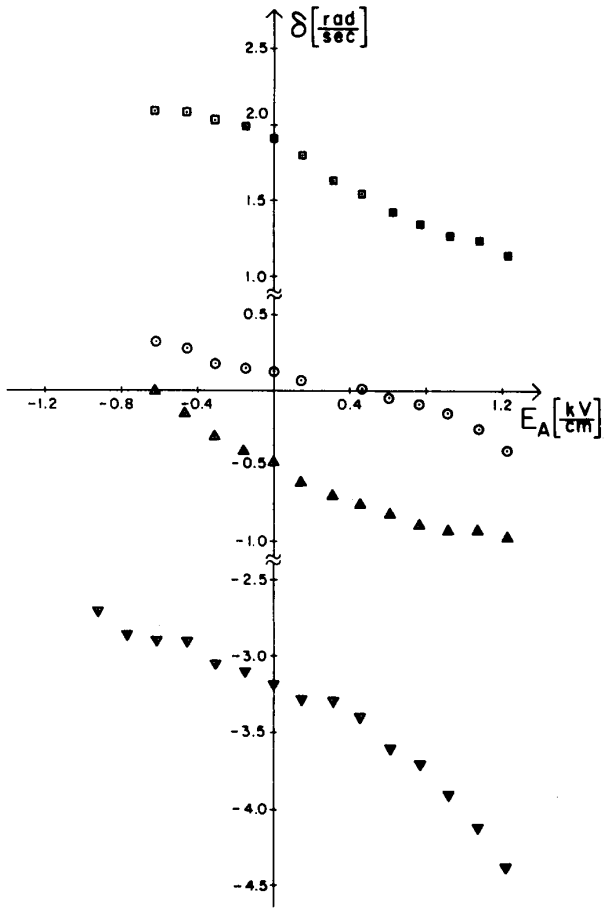

Fig. 8. Measured detuning in the ring PPCM versus applied dc field.

III. The Double Color Pumped Oscillator and the Double Phase Conjugate Mirror

A. Background

The realization of wave mixing and phase conjugation with low-power light beams spurred interest in the use of photorefractive crystals for real-time image processing [48]. These crystals can display real-time adaptability and amplification. However, since the wave mixing configuration is identical to that of regular holography, the Bragg condition still limits the angular and spectral flexibility in the reading beam. In addition, the mandatory presence of a reference beam coherent with the signal-bearing beam makes this device unsuitable, for example, in remote processing tasks.

These limitations are not shared by PPCM's. Here the wave mixing occurs automatically by simply pumping the crystal with the signal beam. For this reason, however, a PPCM cannot supply gain to the phase conjugate signal. Another basic feature shared by all PPCM's is that the complete signal information is reflected. That is, the crystal acts as a "mirror" for the spatial, intensity, and phase characteristics of the signal beam, as well as the incoming photons themselves.

These features, however fundamental they may seem, are not shared by the DPCM and double-color pumped oscillator (DCPO). These devices, which we have recently demonstrated [12]–[16], are shown in Fig. 1. Two beams (beams 4 and 2 in the figure), which need not be mutually coherent nor of the same wavelength, interact to build up a bidirectional holographic link in a photorefractive crystal. Both beams can carry separate spatial, temporal, and phase information. Through this interaction, each input beam loses its own spatial characteristics and picks up the spatial profile of the other counterpropagating input beam as it advances through the crystal. The input beams find each other in a "handshaking" fashion, and are self-bent into each other to produce the oscillation beams 1 and 3. This is accompanied by the build up of gratings in the crystal. The grating set is written simultaneously by the interference of beams 4 with its self-deflected beam 1 and similarly, 2 and 3. Therefore, a self-consistent solution exists: a single, coherent grating set written by and mutually supporting two beam pairs of different wavelengths.

In the degenerate case (identical wavelengths for inputs 4 and 2), the output beams 3 and 1 are the phase conjugate of 4 and 2 respectively, forming a DPCM. In the nondegenerate case, the beams exit the crystal with an angular offset θ. This is a manifestation of the internally generated solution for Bragg matching. We summarize the salient features of these devices, which set them apart from other photorefractive oscillators and phase conjugate mirrors.

1) The crystal is pumped by two completely independent beams. This allows for remote processing tasks, without the need for a mutually-coherent reference source.

2) The Bragg condition is automatically self-satisfied (as an oscillation condition) for any combination of input wavelengths. As a result, the spectral and angular tolerances are not dictated by this strict, fundamental constraint which is present in regular volume holography. Rather, the material (photorefractive) properties of the crystal determine a much wider bandwidth of operation. These properties, in principle, can be tailored to meet specific requirements.

3) In the DPCM, both input beams can carry complex spatial information. Each spatial profile is completely phase conjugated, without carrying any image crosstalk from the other input beam. In regular holography or four-wave mixing, any spatial information on the pumps degrades the fidelity of the phase conjugate output due to crosstalk. The DCPO favors complex spatial information on only one of the beams.

4) The input beams exchange their spatial structure. However, since the photons themselves are transmitted, the other characteristics of each beam are retained and transmitted through the crystal. *This includes intensity, phase, and polarization modulation.* Referring to Fig. 1(g), beam 3 (1) will carry the phase conjugate image of input beam [4] (2), but will otherwise behave like input beam 2 (4).

5) Reflectivity amplification is possible, unlike other

PPCM's, due to the use of two input beams. This will allow a fan-out capability.

These are the essential ingredients for a dynamic, bidirectional holographic interconnect [49].

B. Amplification and Reflectivity in the Double Phase Conjugate Mirror

An analysis of the DPCM has shown that the intensity of the phase conjugate outputs can be greater or less than their corresponding inputs [12], [14]. This depends upon the strength of the coupling constant for the crystal, and the ratio of the input intensities. Referring to Fig. 1, the boundary conditions for the complex amplitudes A_i of the beams at the crystal faces are $A_4(z = 0) = A_4(0)$, $A_2(z = l) = A_2(l)$, and $A_1(0) = A_3(l) = 0$. All quantities can be expressed by the input beam ratio $q = I_4(0)/I_2(l)$. The conserved normalized power density flux Δ, defined in (10a) (and normalized by I_0), is given here by $\Delta = (1 - q)/(1 + q)$. The complex amplitude transmissivities for each of the counterpropagating beam channels in the crystal have been shown above [see (19)] to be the same in both directions. An expression for the symmetric intensity transmission $T = I_3(0)/I_2(l) = I_1(l)/I_4(0)$ is given by

$$T = \frac{a^2[q^{-1/2} + q^{1/2}]^2 - [q^{-1/2} - q^{1/2}]^2}{4} \quad (28)$$

where a is related to the coupling coefficient γ by

$$\tanh\left(-\frac{\gamma l}{2} \cdot a\right) = a. \quad (29)$$

We find for the reflectivities of the device $R_0 = I_3(0)/I_4(0)$ and $R_l = I_1(l)/I_2(l)$ that

$$R_0 = T/q \qquad R_l = Tq. \quad (30)$$

Equations 28 and 29 give the lowest threshold possible for γl, $|(\gamma l)_t| = 2$. From (28) we see that for $q = 1$ the transmission is maximum and equal to a^2. The range of q for oscillation is

$$\frac{1 - a}{1 + a} < q < \frac{1 + a}{1 - a}. \quad (31)$$

The DPCM can exhibit a maximum reflectivity $R_{\max}$ greater than one, and a range of q in which this reflectivity amplification occurs. From (28) and (30),

$$R_{\max} = \frac{a^2}{1 - a^2} \quad (32)$$

at $q^{\pm 1} = (a^2 + 1)/(1 - a^2)$, and is greater than 1 for $a \geq 1/\sqrt{2}$, or $|\gamma l| > 2.49$. For example, for a crystal with $|\gamma l| = 3$, $R_l = R_{\max} = 2.8$ at $q = 6.61$. These equations neglect the effect of absorption in the crystal, which might decrease the transmission and reflection considerably.

In an experiment, the 488 nm line output of an argon ion laser running in multimode (without an etalon), having extraordinary polarization, was split into two input beams 4 and 2. These beams were loosely focused into opposite faces of the same $BaTiO_3$ crystal to form a DPCM. The angle between the input beams 4 and 2 inside the crystal was approximately 173°. These beams were not mutually coherent inside the crystal, to ensure that they would not write interfering reflection gratings.

The input intensity ratio q was varied over the entire operating range of the device. In Fig. 9(a), we plot the measured transmission to both sides of the crystal, after accounting for Fresnel reflections at the cuvette and crystal interfaces. $T_{0\to l} \equiv I_1(l)/I_4(0)$ is the transmissivity of the oscillation beam from the crystal face $z = 0$ to $z = l$, and $T_{l\to 0} \equiv I_3(0)/I_2(l)$ is the transmissivity of the other oscillation beam in the reverse direction. According to theory, the DPCM is perfectly symmetric so that $T_{0\to l} = T_{l\to 0} = T$. These curves display that symmetry, within experimental error. This symmetry is also seen in the measured reflectivity curves of Fig. 9(b). Note the reflectivity amplification of about 4 for this crystal. From the experimental curves, the value of $|\log q|$ at the onset of oscillation is about 1.7, and approximately 1.2 at the reflectivity peak. Using (29) and (31), this first data point indicates that $\gamma l = -4.07$ for this crystal. Using the data point at the reflectivity peak, (29) and (32) point to $\gamma l = -3.7$. The deviation between these two values can be attributed to absorption in the crystal and experimental error. Absorption also seems to have a significant effect on the scaling of these curves. For $\gamma l = -3.7$, theory predicts a maximum reflectivity of 7.6, or almost double the measured value. Fig. 10(a) and (b) display theoretical graphs of DPCM transmission and reflection for various γl. A similar value of $|\gamma l|$ (≈ 3.5–4) was measured for this crystal in a two beam coupling amplifier scheme. However, firm comparisons cannot be made, since γl is dependent upon the crystal's orientation and interaction length l, and varies for different configurations.

C. Spatial Modulation and Filtering in the DPCM and other Photorefractive Oscillators

We have discussed and demonstrated the use of the DPCM as a bidirectional spatial light modulator, and have shown that this two-way information encoding occurs without crosstalk [50]. That is, output 1, although derived from input 4, carries none of that input's information. Similarly, output 3 is derived from input 2 but bears no resemblance to that input.

Other photorefractive oscillators exhibit similar features. The phase conjugating capability of the ring PPCM is based on the lack of crosstalk. Although the feedback pump through the ring configuration is carrying the image of the signal it does not deteriorate the phase conjugation. In the semilinear PPCM the common belief attributed the phase conjugating capability to the cleaned-up self-generated pumps. Experiments involving oscillators with image-bearing pumps in the two cascaded semilinear PPCM's rules out this explanation [51]. The self-generated pumps were spatially modulated, but phase conjugation was still obtained. An image-bearing oscillator with

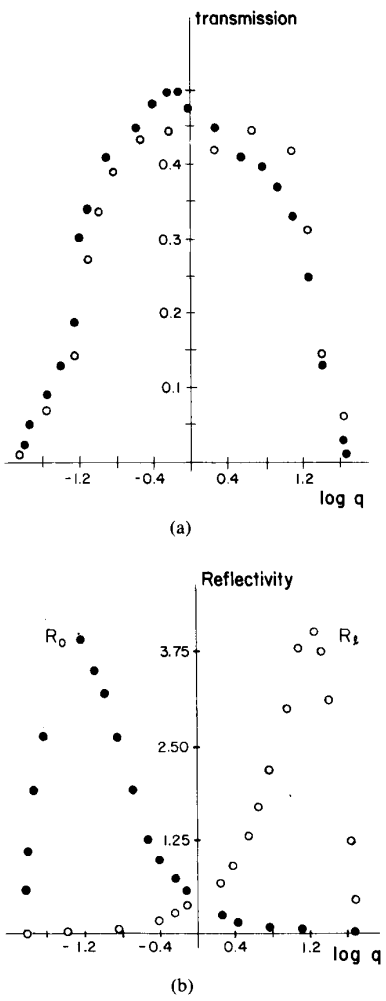

Fig. 9. (a) Measured transmission $T_{0\to l}$ and $T_{l\to 0}$ in the DPCM versus log (q), where q = input beam intensity ratio. (b) Measured reflectivities R_o and R_l in the DPCM versus log q. Note the maximum reflectivity amplification of about 4, for this crystal.

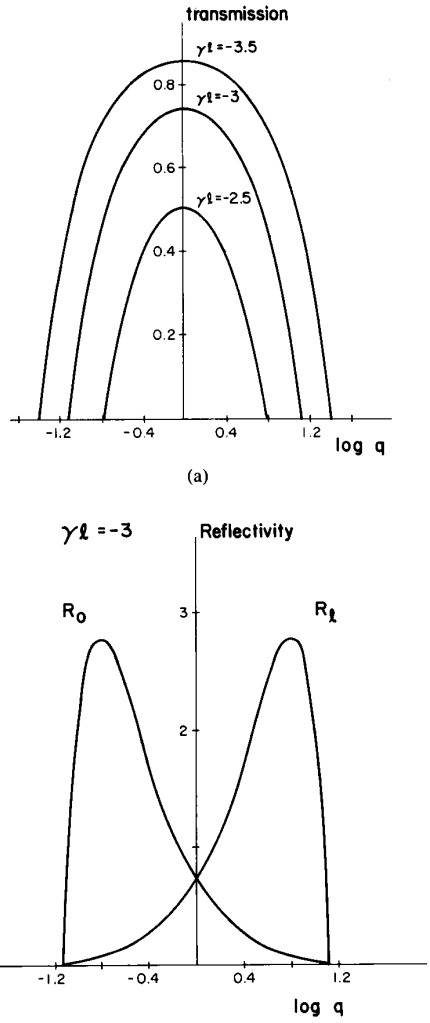

Fig. 10. Theoretical plots of transmissivity (a) and reflectivity (b) in the DPCM.

a two-facing DPCM exhibited similar isolation features where the external input pumps for the DPCM's and the oscillation between them were carrying images [12]. From the point of view of holography, image crosstalk of the interacting beams is expected [50]. Reading a hologram with one of the image-bearing writing beams or its phase conjugate causes crosstalk on the diffracted output beam. Experimental evidence shows, however, the absence of significant crosstalk in the various photorefractive oscillators. The explanation for this interesting behavior was given in [50] and is briefly reviewed here. The key to understanding the operation of the DPCM, DCPO, and other devices lies in the word "oscillation." In the externally-pumped phase conjugate mirror (Fig. 2), the grating is externally written by beams 4 and 1. One must externally care for the Bragg condition, by inputting beam 2 properly so that $\vec{k}_2 = -\vec{k}_1$. If this condition is not met, as is the case when beam 2 is not counterpropagating with respect to beam 1, then the output beam 3 might still appear but is a lower intensity due to the phase mismatch, and is not the phase conjugate of input 4. This situation has practical applications, such as the real-time convolution and correlation experiments that have been done in the past [52]. These effects actually depend upon crosstalk for their operation. In the DPCM, a grating is not externally imposed. It builds up as an oscillation, with the emergence of two output beams, in response to the presence of two inputs. From the gain point of view it is straightforward to realize the preference of phase conjugate pairs. This results in the maximum photorefractive gain due to the overlapping of two sets of gratings. In the four-wave scheme the sum of the amplitudes of the two sets of transmission gratings, induced by the beams couples (A_1A_4) and (A_2A_3), is proportional to $A_1A_4^* + A_2^*A_3$ + c.c., where c.c. stands for the complex conjugate terms. If the counterpropagating beams are phase conju-

gate beams (i.e., $A_1 \propto A_2^*$ and $A_3 \propto A_4^*$) the terms overlap in space. It permits the mutual strengthening and buildup of the two sets of gratings and the self generated beams, and gives the highest photorefractive gain.

From (1), the solution for the self-generated beams 1 and 3 in the DPCM and DCPO is $\vec{k}_1 - \vec{k}_3 = \vec{k}_4 - \vec{k}_2$.

This k-vector relation describes a conus of oscillation beams out of the xz plane, since the only constraint is the vector $\vec{k}_4 - \vec{k}_2$ [11]. In certain experimental conditions, these cones of light form as the outputs of the DPCM and DCPO. This may occur, for example, in a crystal with low photorefractive efficiency, or for input beams with a relatively broad waist in the crystal. This solution, although not the phase conjugate one, is still possible. The situation changes, however, when information is inserted onto at least one of the input beams. In this case, the only solution is phase conjugation. Spatial information in the inputs helps to "tie down" the oscillation by presenting added constraints. It appears that these oscillators have an affinity for spatial information. This effect has been observed experimentally. A similar situation appears to exist in SBS (stimulated Brillouin scattering) wave mixing, where an abberated input beam helps to increase the phase conjugate fidelity [53].

The optimization of the grating writing may still suffer from information crosstalk in the reading stage as described above. Since the distorted diffracted beam itself participates in writing the very same gratings, it can lead to an iterative walk-off from the phase conjugate solution and wash out of the gratings. The volume grating's selectivity in photorefractive oscillation restricts this walk off. This can be understood by describing the image bearing beams as an integral of plane waves with slightly different directions. These components are represented by waves A_2 and $A_{2'}$ for beam 2 of the DPCM in Fig. 11. Crosstalk arises where one plane wave component (say $A_{2'}$ is diffracted by the gratings written by another component (A_2 or its phase conjugate beam A_1), and vice versa. A basic filtering mechanism in the oscillators eliminates such diffractions.

The filtering effect was analyzed for the DPCM [50]. We consider the simple scheme of Fig. 11 in which beam 2′ (replaces 2) is misaligned with respect to beam 1, such that their wave vectors $\bar{k}_1 + \bar{k}_{2'} = \overline{\Delta k} \neq 0$. This is still a four-wave mixing configuration with a phase mismatch $\overline{\Delta k}$, which will show the angular selectivity of the mixing process.

The coupled wave equations for beams 1 and 3 in the nondepleted pumps (beams 2′ and 4) approximation for transmission gratings and negligible absorption, are

$$\frac{dA_1}{dz} = -\frac{\gamma}{I_0}\left[|A_4|^2 A_1 + (A_2^* A_4)A_3 e^{-i\Delta k_z z}\right]$$

$$\frac{dA_3}{dz} = \frac{\gamma}{I_0}\left[|A_2|^2 A_3 + (A_2 A_4^*)A_1 e^{i\Delta k_z z}\right] \qquad (33)$$

where the prime of 2′ is omitted, $I_0 \approx I_2 + I_4$, and Δk_z is the component of $\overline{\Delta k}$ along the z axis. For $\overline{\Delta k} = 0$, the full nonlinear problem is exactly solvable.

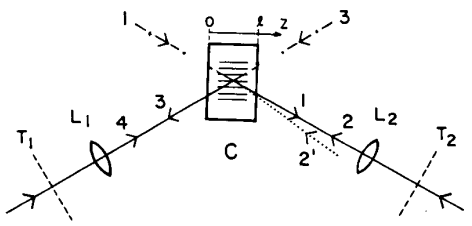

Fig. 11. Schematic of the DPCM with two plane wave components 2 and 2′ representing the input image T_2.

With the boundary conditions $A_1(z = 0) = A_1(0)$ and $A_3(z = l) = 0$, we obtain from [33]

$$\begin{cases} \rho \equiv \dfrac{A_3(0)}{A_1(0)} = -\dfrac{\gamma(A_4^*/A_2^*)}{(1+q)} \cdot \dfrac{\sinh(sl)}{s\cosh(sl) + (1/2)(\gamma - i\Delta k_z)\sinh(sl)} \\ t \equiv \dfrac{A_1(l)}{A_1(0)} = \dfrac{s\exp[(p\gamma - i\Delta k)l/2]}{s\cosh(sl) + (1/2)(\gamma - i\Delta k_z)\sinh(sl)} \end{cases} \qquad (34)$$

where $s = (1/2)[p^2\gamma^2 - 2\gamma(i\Delta k_z) - (\Delta k_z)^2]^{1/2}$, $p = (1-q)/(1+q)$, and $q = I_4/I_2$. For $\overline{\Delta k} = 0$, (34) becomes

$$\rho = -\left(\frac{A_4^*}{A_2^*}\right)\frac{e^{p\gamma l} - 1}{(e^{p\gamma l} - q)} \qquad t = \frac{e^{p\gamma l}(1-q)}{(e^{p\gamma l} - q)}. \qquad (35)$$

The infinities of ρ and t permit the self-buildup of beams 1 and 3 and give the operating points of the DPCM, since zero $A_1(0)$ and $A_3(l)$ build up into nonzero output $A_1(l)$ and $A_3(0)$. Thus, our approximate method predicts the operation of the DPCM even for real γ (for the common case in photorefractive materials where the phase shift between the induced gratings and the fringes is $\pi/2$). The oscillation ($\rho = t = \infty$) occurs at

$$\gamma l = (\ln q)(1+q)/(1-q) \qquad (36)$$

for $\overline{\Delta k} = 0$. The threshold value of the coupling constant is $|\gamma l|_{\text{th}} = 2$, for the pump ratio $q = 1$. When q approaches 0 or ∞, the needed γl increases to ∞. This is in agreement with the exact theory. It also predicts the boundaries of the operable q region, as given by the exact calculation in (31). The only difference is the specific relation between (γl) and q for oscillation. Similar results can be derived for the ring PPCM, which is also described by (34) with the appropriate boundary conditions.

The results of (34) for the DPCM resemble those of DFB (distributed feedback) laser [54] and the standard ex-

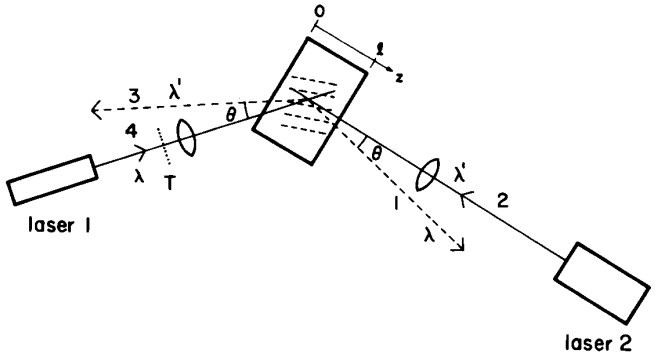

Fig. 12. Experimental schematic of the double-color pumped oscillator (DCPO) for beam steering and image color conversion.

ternally pumped four-wave mixing with phase mismatch [11]. A basic difference is that in the latter cases oscillation is possible only for $\Delta k \neq 0$ or a nonreal coupling constant. In the DFB laser this dictates a detuning from the frequency that matches the Bragg condition. In the DPCM, however, oscillation is achievable for $\Delta k = 0$. We also note that in all photorefractive wave mixing configurations, but not in the DFB laser, the effective coupling parameters are dependent on the pump intensity ratio. Since small deviations of Δk from zero cause a drastic decrease of ρ and t [55], oscillation is restricted to $\Delta k = 0$. Large Δk, which might have allowed an oscillation condition as in the DFB laser [54], is not relevant here because of the deterioration of the effective gain which is optimized for phase conjugate beams.

Since its operation is based on the oscillation and self-buildup of beams, 1, 3, and the gratings, a complete phase matching and phase conjugation is needed in the DPCM. This dictates the elimination of cross diffractions. Similar arguments hold for other photorefractive oscillators. Thus the ring and semilinear PPCM also involve crosstalk elimination and buildup of phase conjugate beams.

D. Analysis of the Double-Color Pumped Oscillator

The DCPO, shown in Figs. 1 and 12, is an extension of the DPCM to nondegenerate wavelengths. This was the first demonstration to our knowledge of a photorefractive oscillator whose operation involves two input beams of different colors, and automatically fulfills the Bragg matching condition for any pair of wavelengths [15], [16].

The threshold value of γl for oscillation as well as the effect of nondegenerate wavelengths were analyzed using the nondepleted pumps approximation. As shown above, this involves two equations for the oscillation beams 1 and 3:

$$\frac{dA_1}{dz} = \frac{-\gamma}{I_0}(A_4A_4^*)A_1 - \frac{u\gamma}{I_0}(A_2^*A_4)A_3 \tag{37}$$

$$\frac{dA_3}{dz} = \frac{v\gamma}{I_0}(A_2A_4^*)A_1 + \frac{(uv)\,\gamma}{I_0}(A_2A_2^*)A_3 \tag{38}$$

The difference in the grating writing (or refractivity) with wavelength λ' (beams 2 and 3) compared to λ (of 4 and 1) is manifested in the second terms of (37) and (38), through u, where

$$u = \left(\frac{n_g(\lambda')}{n_g(\lambda)}\right)\left(\frac{\exp\left[-i\phi_g(\lambda')\right]}{\exp\left[-i\phi_g(\lambda)\right]}\right).$$

The wavelength nondegeneracy in the grating's reading stage is expressed in the extra factor of v in (38)

$$v = \left(\frac{\lambda}{\lambda'}\right)\left(\frac{\cos\alpha}{\cos\alpha'}\right)$$

where α and α' are the angles between beams 1 and 3, respectively, and the crystal's surface ($z = l$) normal. The coupling constant γ corresponds to α and λ.

The solution for A_1 and A_3 where the pumps A_2 and A_4 are taken to be constants (nondepleted), gives ρ and t, where

$$\rho \equiv A_3(0)/A_1(0) = \frac{-1}{u}\left(\frac{A_4}{A_2}\right)^* \frac{e^{p\gamma l} - 1}{e^{p\gamma l} - q/(uv)} \tag{39}$$

$$t \equiv A_1(l)/A_1(0) = \frac{e^{p\gamma l}\left[1 - q/(uv)\right]}{e^{p\gamma l} - q/(uv)} \tag{40}$$

where $q \equiv |A_4/A_2|^2$ is the input pumps' intensity ratio, and $p \equiv (uv - q)/(1 + q)$. For an operating DCPO, ρ and t are infinite, since zero beam amplitudes for $A_1(0)$ and $A_3(l)$ grow into nonzero $A_1(l)$ and $A_3(0)$ output beams. At this operating point [from (39) or (40)]

$$\gamma l = (1/p)\ln\left[(q/uv)\right]. \tag{41}$$

The threshold value for γl, which is the lowest operable value, is derivable from (41). This occurs at

$$\left|(\gamma l)_{\text{th}}\right| = 1 + 1/(uv) \text{ at } q = uv. \tag{42}$$

For the DPCM (the degenerate case) $uv = 1$ and the correct values are obtained, i.e., $|(\gamma l)_{\text{th}}| = 2$ and $q = 1$.

These equations show that there are no basic restrictions on the operation of the DCPM with any two input

frequencies λ and λ'. The only requirement for $|\gamma l|$ is that it not be less than the $|(\lambda l)_{th}|$ derived above. In $BaTiO_3$, $|(\gamma l)|$ is sufficiently high throughout the visible spectrum including the near infrared [56].

As described in the previous section, the output beams in the DCPO are angularly deflected with respect to the inputs. An analysis of this deflection was done [15] with the help of Fig 13, which describes the geometry of the beams inside the crystal. The input parameters are the wave vectors of the pumps $\bar{k}_4$ and $\bar{k}_2$ and the angle ψ between them. In addition, we know the vector magnitudes $k_1 = k_4 \equiv k = 2\pi/\lambda$ and $k_3 = k_2 \equiv k' = 2\pi/\lambda'$. The direction of the wave vectors of the self-generated beams $\bar{k}_1$ and $\bar{k}_3$ are self-chosen through the oscillation such that a common grating $\bar{k}_g = \bar{k}_4 - \bar{k}_1 = \bar{k}_2 - \bar{k}_3$ is produced. Thus,

$$k_g = 2k \sin(\phi/2) = 2k' \sin(\phi'/2). \tag{43}$$

This results in the following expression for the beam deflection θ inside the crystal:

$$\theta = (\phi - \phi')/2 = \tan^{-1}\left(\frac{\sin\psi}{(\lambda'/\lambda) - \cos\psi}\right) - \tan^{-1}\left(\frac{\sin\psi}{(\lambda/\lambda') - \cos\psi}\right). \tag{44}$$

For small changes of λ' around λ, this gives

$$d\theta = -\sin\psi\left(\frac{d\lambda}{\lambda}\right). \tag{45}$$

In our experiments $\psi \approx 173°$, hence $d\theta \approx 0.12(d\lambda/\lambda)$ in radians. Outside the crystal this angle is magnified due to refraction by a factor on the order of the crystal's refractive index (~ 2.4). A further increase may be achieved for ψ close to 90°.

E. Self-Bragg Matched Beam Steering and Image Color Conversion

In an experimental demonstration of the DCPO which we carried out recently [16], we used a single domain $BaTiO_3$ crystal with similar geometry to and orientation as the DPCM. We pumped the crystal with two beams 4 and 2, each of a different color, chosen from the extraordinarily-polarized spectrally-separated output lines of an Argon ion laser operating on its five strong lines: 514.5, 496.5, 488, 476.5, and 457.9 nm, as well as the 632.8 nm line of a HeNe laser. Oscillation and efficient self-generation of beams 1 and 3 was achieved with every combination of two lines. As shown in Fig. 12, one of the pumps (beam 4) with wavelength $\lambda = 488$ nm was spatially modulated by a resolution chart T and then focused ($f = 10$ cm) into the crystal face $z = 0$. Each of the argon laser's 5 lines took a turn as beam 2, which was focused ($f = 20$ cm) through the crystal face $z = l$, and crossed beam 4 in the crystal, with the same angular configuration used for each line. The c axis is parallel to the z axis in the figure. The image transferred from beam 4 to beam 3, with the color of pump beam 2, is shown in the series of pictures in Fig. 14. As shown in Fig. 12, this was accompanied by angular deflection of beams 3 and 1. Each picture in Fig. 14 corresponds to a different wavelength of beam 2 (and 3). The transferred image quality in beam 3 for λ and λ' far part will deteriorate. The need to simultaneously Bragg match all of the spatial components of the grating puts an upper limit on the number of resolution elements that can be processed for $\lambda \neq \lambda'$ [57]. Besides the decrease in resolution, another important factor is the difference in crystal efficiency for the two input wavelengths. As we have shown earlier, this efficiency is a function of wavelength-dependent material parameters and the input pumps' intensity ratio. However, the DCPM using $BaTiO_3$ should be useful for infrared to visible image color conversion. We have recently observed IR (0.8 nm) to visible (HeNe and argon ion lines) image conversion.

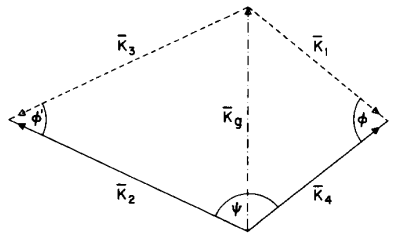

Fig. 13. k vector diagram of the wave mixing in the DCPO. The inputs are beams 2 and 4 with the angle ψ between them in the crystal. Beams 3, 1, and the grating (represented by $\bar{k}_g$) build up as an oscillation.

The DCPO operated even when one or both input pumps consisted of the complete (unseparated) all-lines output of the argon laser. In particular, when input beam 4 contained all lines and was spatially modulated, inputting beam 2 at any wavelength λ' within the argon spectrum resulted in efficient oscillations and a spatially-modulated output beam 3. In this case, output beam 1 was seen to contain mainly the two strongest argon lines at 488 and 514.5 nm.

A deflection of beam 1 at the crystal output $z = l$ occurred in conjunction with the image color conversion at $z = 0$. We studied the beam deflection of output beam 1, which had a constant $\lambda = 488$ nm. Fig. 15 shows this deflected output beam and corresponding θ values for each color of beam 2. The deflection range in this experiment was about 5.7° for a λ' tuning range of 174.9 nm. This value agrees with (44) and (45). As for beam 3, high diffraction efficiencies for beam 1 were observed, varying from 30 to 60 percent for λ' within the argon lines and about 6 percent for $\lambda' = 632.8$ nm.

In conventional beam steering devices, little control can be exercised in modifying the beam's spatial profile. In some applications, it may be important to spatially modulate as well as deflect a beam. The DCPO is unique in that it integrates these two characteristics while it automatically optimizes the efficiency, as explained earlier. Referring to Fig. 12, output beam 3 at λ', derived from

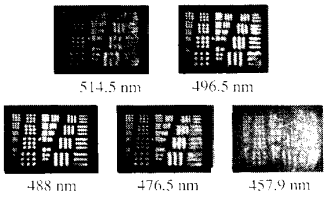

Fig. 14. Image color conversion in the DCPO. These images, with the wavelength noted, were carried on output beam 3 of Fig. 12.

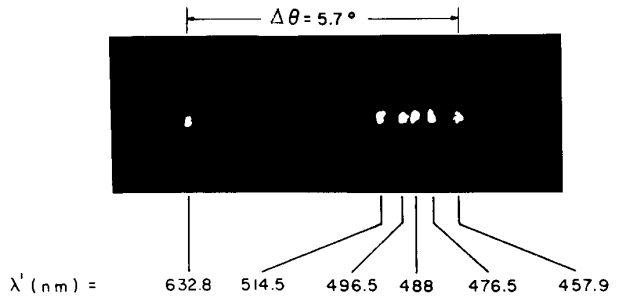

Fig. 15. Beam steering in the DCPO. Deflected output beam 1 at 488 nm is shown for varying λ'.

pump 2, takes on the spatial information of pump 4 at λ as it is deflected. Varying λ in this case (and not λ') will change the deflection angle of this modulated output beam.

Two other configurations which allow incoherent beam coupling have recently been demonstrated [58], [59]. Both are actually variations of the two-facing DPCM (2F-DPCM) resonator [12] which can form in a single crystal. One involves two internal reflections [58], and the other a single internal reflection [59] at crystal faces. Unlike the DPCM, these configurations are probably not easily extendable to nondegenerate wavelengths. The angular offset θ of the DCPO would cause an internal walk-off from the two interaction regions. In the 2F-DPCM resonator with two crystals [12], this walk-off can be prevented, by imaging one interaction region onto the other with a lens in the resonator cavity. In this fashion, the resonator can be pumped with nondegenerate input beams.

F. Other Applications for the DCPO/DPCM

We envision a multitude of uses for the DPCM and DCPO, which fall into one of the following categories: holographic interconnects, image processing and spatial light modulation, beam steering, and interferometry.

An example of a DPCM/DCPO based optical interconnect which we have recently suggested [60] is shown in Fig. 16. The links between the beams, which can carry intensity, phase, or polarization modulation, form dynamically. Any intensity or polarization modulation rate must be greater than the inverse of the photorefractive response time τ. At nominal power levels, $\tau \geq 1$ ms so that any modulation above 10 KHz would be transmitted without affecting the photorefractive gratings [14], [60], [61].

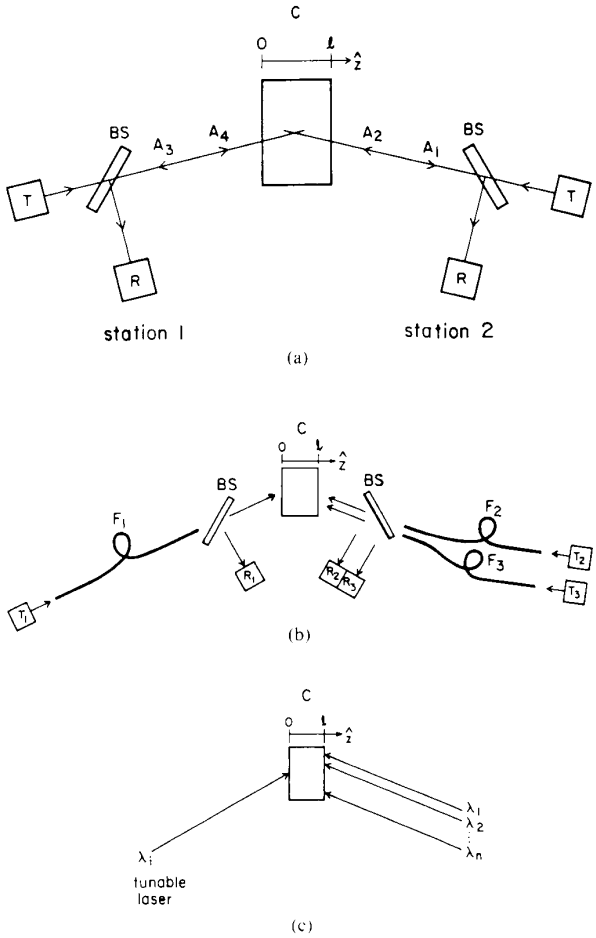

Fig. 16. Optical interconnect schemes with the DPCM. (a) Bidirectional transmitting–receiving scheme. T: transmitter, R: receiver, BS: beamsplitter. (b) An experimental interconnection scheme [60]. The beams guided in the fibers can be of different wavelength combinations, depending upon the desired communication mode, such as broadcasting, point-to-point, or wavelength division multiplexing. (c) Point-to-point interconnect. The beam from the left-hand side of the crystal, with a tunable wavelength λ_i, can be tuned to link with any of the wavelengths from the right-hand side of the crystal.

Phase modulation can be at any rate, since we have shown that uniform spatial phase changes do not affect the grating structure. Since the DPCM generates phase conjugate beams, these links can be formed through multimode fibers or other aberrations [12]–[14]. We have demonstrated various interconnect schemes between two arrays of fibers [60].

With the DPCM or DCPO, lasers (laser diodes, for example) can be coupled to form a coherent communication link, even through multimode fibers [13], [62]. Under certain circumstances laser can be phase locked, through optimum light injection via the DPCM channel [13]. This has importance beyond communication-based applications.

In the realm of image processing, we have demonstrated image (or wavefront) exchange between mutually incoherent (and in the DCPO, nondegenerate) beams

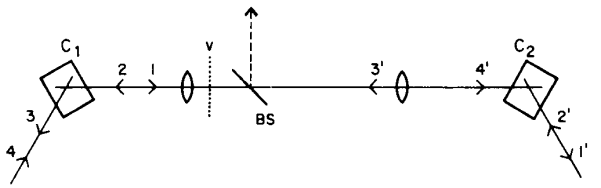

Fig. 17. The two-facing DPCM resonator [12], [14]. The image V is supported in the resonator cavity.

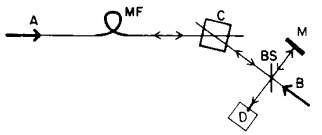

Fig. 18. Beam clean-up as well as coherent communication scheme between two sources A and B. The DPCM matches the received wavefronts to the local laser B. This configuration was used in [13] for the beam clean-up of A, as well as for interferometry.

[12]–[16]. This has applications in beam cleanup, controllable spatial light modulation, image color conversion, wavefront matching, and other adaptive optics schemes. The gain and threshold properties of the DPCM have been applied to edge detection (or spatial bandpass filtering) and gray level discrimination [14]. We have also demonstrated photorefractive resonators incorporating two PPCM's [51], and the 2F-DPCM [12] (shown in Fig. 17), which can support pictorial information in the oscillation beams. This may be useful in realizing iterative algorithms found in phase retrieval, super-resolution, associative memories, and neural networks [14].

The beam-steering ability of the DCPO was reviewed above. Its main advantage is a potentially large angular deflection range, not affected by the usual Bragg condition.

Combining the beam cleanup and phase transmission properties of the DPCM, we have demonstrated a Mach–Zehnder interferometer with multimode fibers in the interferometer arms [13]. This configuration, which is extendable to nondegenerate wavelengths using the DCPO, would also be useful for coherent communications through aberrating media. This can be accomplished by matching the wavefronts of a detected remote light source with a local light oscillator, as shown in Fig. 18. In general, these schemes provide a means for mutually controlling the shape and spatial modulation of two (or more) light beams.

IV. Conclusions

This paper has tried to lead to a deeper understanding of the dynamics of self-frequency detuning in photorefractive oscillators. Its dependence upon optical phases and electric fields can be used to devise "active" interferometric sensors, where optical phase is translated into a frequency detuning. These effects are intimately interconnected with the presence of an internal electric field, shown to exist in $BaTiO_3$.

Two or more completely independent laser beams can join together to form a mutual, coherent photorefractive oscillation. The obvious implications of this new effect for beam manipulation and control schemes are far reaching, with applications in dynamic interconnects, beam steering, image processing, and interferometry.

The research of photorefractive devices and applications has surged far ahead of material science research in this area. This presents the main bottleneck which is preventing the transition of these devices from the laboratory to industry. The search is on for photorefractive crystals, dopants, and other optimum operating conditions to achieve good optical quality crystals with high efficiency and sensitivity and fast response time.

Since the first reports on the "damaging" effects of photorefractivity, a multitude of optical manipulations with low light intensities have been demonstrated. These materials may emerge as one of the victors in the struggle to domesticate the photon.

Acknowledgment

The authors wish to thank Z. Shehory for his technical help.

References

[1] For reviews, see D. H. Auston *et al.*, "Research on nonlinear optical materials: An assessment," *Appl. Opt.*, vol. 26, pp. 211–234, 1987; and *Opt. Eng.*, vol. 26, no. 1, Jan. 1987 and *Opt. Eng.*, vol. 26, no. 5, 1987.

[2] *Optical Phase Conjugation*, R. A. Fisher, Ed. New York: Academic, 1983.

[3] A. Yariv, "Phase conjugate optics and real time holography," *IEEE J. Quantum Electron.*, vol. 14, pp. 650–660, 1978.

[4] J. Feinberg and R. W. Hellwarth, "Phase conjugating mirror with continuous wave gain," *Opt. Lett.*, vol. 5, pp. 519–521, 1980.

[5] B. Fischer, M. Cronin-Golomb, J. O. White, and A. Yariv, "Amplified reflection, transmission, and self oscillation in real-time holography," *Opt. Lett.*, vol. 6, pp. 519–521, 1981.

[6] J. O. White, M. Cronin-Golomb, B. Fischer, and A. Yariv, "Coherent oscillation by self-induced gratings in the photorefractive crystal $BaTiO_3$," *Appl. Phys. Lett.*, vol. 40, pp. 450–452, 1982.

[7] M. Cronin-Golomb, B. Fischer, J. Nilsen, J. O. White, and A. Yariv, "Laser with dynamic holographic intracavity distortion correction capability," *Appl. Phys. Lett.*, vol. 41, pp. 219–220, 1982.

[8] M. Cronin-Golomb, B. Fischer, J. O. White, and A. Yariv, "Passive (self-pumped) phase conjugate mirror: Theoretical and experimental investigation," *Appl. Phys. Lett.*, vol. 41, pp. 689–691, 1982.

[9] J. Feinberg, "Self-pumped, continuous wave phase conjugator using internal reflections," *Opt. Lett.*, vol. 7, pp. 486–488, 1982.

[10] M. Cronin-Golomb, B. Fischer, J. O. White, and A. Yariv, "Passive phase conjugate mirror based on self-induced oscillation in an optical ring cavity," *Appl. Phys. Lett.*, vol. 42, pp. 919–921, 1983.

[11] ——, "Theory and application of four-wave mixing in photorefractive media," *IEEE J. Quantum Electron.*, vol. QE-20, pp. 12–30, 1984.

[11a] R. A. McFarlane and D. G. Steel, "Laser oscillator using resonator with self-pumped phase conjugate mirrors," *Opt. Lett.*, vol. 8, pp. 208–210, 1983.

[12] S. Weiss, S. Sternklar, and B. Fischer, "Double phase conjugate mirror: Analysis, demonstration, and applications," *Opt. Lett.*, vol. 12, pp. 114–116, 1987.

[13] S. Sternklar, S. Weiss, M. Segev, and B. Fischer, "Beam coupling and locking of lasers using photorefractive four-wave mixing," *Opt. Lett.*, vol. 11, pp. 528–530, 1986; ——, "Mach Zehnder interferometer with multimode fibers using the double phase conjugate mirror," *Appl. Opt.*, vol. 25, pp. 4518–4520, 1986.

[14] S. Sternklar, S. Weiss, and B. Fischer, "Optical information processing with the double phase conjugate mirror," *Opt. Eng.*, vol. 26, pp. 423–427, 1987.

[15] B. Fischer and S. Sternklar, "Self Bragg-matched beam steering using the double color pumped photorefractive oscillator," *Appl. Phys. Lett.*, vol. 51, pp. 74-75, 1987.
[16] S. Sternklar and B. Fischer, "Double-color-pumped photorefractive oscillator and image color conversion," *Opt. Lett.*, vol. 12, pp. 711-713, 1987.
[17] J. P. Huignard and A. Marrakchi, "Coherent signal beam amplification in two-wave mixing experiments with photorefractive $Bi_{12}SiO_{20}$ crystals," *Opt. Commun.*, vol. 38, pp. 249-254, 1981.
[18] G. C. Valley, "Two-wave mixing with an applied field and a moving grating," *J. Opt. Soc. Amer. B*, vol. 1, pp. 868-873, 1984.
[19] K. R. MacDonald and J. Feinberg, "Enhanced four-wave mixing by use of frequency shifted optical waves in photorefractive $BaTiO_3$," *Phys. Rev. Lett.*, vol. 55, pp. 821-824, 1985.
[20] W. B. Whitten and J. M. Ramsey, "Self-scanning of a dye laser due to feedback from a $BaTiO_3$ phase-conjugate reflector," *Opt. Lett.*, vol. 9, pp. 44-46, 1984.
[21] F. C. Jahoda, P. G. Weber, and J. Feinberg, "Optical feedback, wavelength response, and interference effects of self-pumped phase conjugation in $BaTiO_3$," *Opt. Lett.*, vol. 9, pp. 362-364, 1984.
[22] J. Feinberg and G. D. Bacher, "Self-scanning of a continuous-wave dye laser having a phase-conjugating resonator cavity," *Opt. Lett.*, vol. 9, pp. 420-422, 1984.
[23] M. Cronin-Golomb, B. Fischer, S. K. Kwong, J. O. White, and A. Yariv, "Nondegenerate optical oscillation in a resonator formed by two phase conjugate mirrors," *Opt. Lett.*, vol. 10, pp. 353-355, 1985.
[24] H. Rajbenbach and J. P. Huignad, "Self induced coherent oscillations with photorefractive $Bi_{12}SiO_{20}$ amplifier," *Opt. Lett.*, vol. 10, pp. 137-139, 1985.
[24a] J. F. Lam, "Origin of phase conjugate waves in self-pumped photorefractive mirrors," *Appl. Phys. Lett.*, vol. 46, pp. 909-911, 1985.
[25] B. Fischer and S. Sternklar, "A new optical gyroscope based on the ring passive phase conjugate mirror," *Appl. Phys. Lett.*, vol. 47, pp. 1-3, 1985.
[26] S. Sternklar, S. Weiss, and B. Fischer, "Controlling the self-frequency shift and intensity of oscillations with photorefractive crystals," *Appl. Opt.*, vol. 24, pp. 3121-3122, 1985.
[27] ——, "Tunable frequency shift of photorefractive oscillators," *Opt. Lett.*, vol. 11, pp. 165-167, 1985.
[28] B. Fischer, "Theory of self-frequency detuning of oscillations by wave mixing in photorefractive crystals," *Opt. Lett.*, vol. 11, pp. 236-238, 1986.
[29] P. Yeh, "Theory of unidirectional photorefractive ring oscillators," *J. Opt. Soc. Amer. B*, vol. 2, pp. 1924-1928, 1985.
[30] A. Yariv and S. K. Kwong, "Theory of laser oscillation in resonators with photorefractive gain," *Opt. Lett.*, vol. 10, pp. 454-456, 1985.
[31] M. Cronin-Golomb and A. Yariv, "Plane wave theory of nondegenerate oscillation in the linear photorefractive passive phase conjugate mirror," *Opt. Lett.*, vol. 11, pp. 242-244, 1986.
[32] L. Solymar and D. J. Cooke, *Volume Holography and Volume Gratings*. New York: Academic, 1981, pp. 164-207.
[33] T. Wilson and L. Solymar, "Two-dimensional coupled differential equations for degenerate four-wave mixing," *Appl. Phys. Lett.*, vol. 38, pp. 669-670, 1981.
[33a] N. V. Kukhtarev, V. B. Markov, S. G. Odulov, M. S. Soskin, and V. L. Vinetskii, "Holographic storage in electro-optic crystals," *Ferroelectrics*, vol. 22, pp. 949-960, 1979.
[34] M. Cronin-Golomb, J. O. White, B. Fischer, and A. Yariv, "Exact solution of a nonlinear model of four-wave mixing and phase conjugation," *Opt. Lett.*, vol. 7, pp. 313-315, 1982.
[35] K. R. MacDonald and J. Feinberg, "Theory of a self-pumped phase conjugator with two coupled interaction regions," *J. Opt. Soc. Amer.*, vol. 73, pp. 548-553, 1983.
[36] S. K. Kwong, A. Yariv, M. Cronin-Golomb, and I. Ury, "Conversion of optical path length to frequency by an interferometer using photorefractive oscillation," *Appl. Phys. Lett.*, vol. 47, pp. 460-462, 1985; and S. K. Kwong, M. Cronin-Golomb, and A. Yariv, "Oscillation with photorefractive gain," *IEEE J. Quantum Electron.*, vol. QE-22, pp. 1508-1523, 1986.
[37] J. C. Diels and I. C. McMichael, "Influence of wave-front-conjugated coupling on the operation of a laser gyro," *Opt. Lett.*, vol. 6, pp. 219-221, 1981.
[38] I. McMichael and P. Yeh, "Self-pumped phase conjugate fiber optic gyro," *Opt. Lett.*, vol. 11, pp. 686-688, 1986.
[39] S. Ezekiel and H. J. Arditty, "Fiber-optic rotation sensors. Tutorial review," in *Fiber Optic Rotation Sensors*, S. Ezekiel and H. J. Arditty, Eds. New York: Springer, 1982, pp. 2-26.
[40] J. P. Jiang and J. Feinberg, "Dancing modes and frequency shifts in a phase conjugator," *Opt. Lett.*, vol. 12, pp. 266-268, 1987.
[41] K. Shiraishi, S. Sugaya, and S. Kawakami, "Fiber faraday rotator," *Appl Opt.*, vol. 23, pp. 1103-1106, 1984.
[42] A. Yariv, *Quantum Electronics*. New York: Wiley, 1975, p. 111.
[43] M. Cronin-Golomb and A. Yariv, "Self-induced frequency scanning and distributed Bragg reflection in semiconductor lasers with phase-conjugate feedback," *Opt. Lett*, vol. 11, pp. 455-457, 1986.
[44] M. C. Gower, "Photoinduced voltages and frequency shifts in a self-pumped phase conjugating $BaTiO_3$ crystal," *Opt. Lett.*, vol. 11, pp. 458-460, 1986.
[45] I. McMichael and P. Yeh, "Phase shifts of photorefractive gratings and phase conjugate waves," *Opt. Lett.*, vol. 12, pp. 48-50, 1987.
[46] A. G. Chynoweth, "Surface space-charge layers in barium titanate," *Phys. Rev.*, vol. 102, pp. 705-714, 1956.
[47] V. M. Fridkin, "The possible mechanism for the bulk photovoltaic effect and optical damage in ferroelectrics," *Appl. Phys.*, vol. 13, pp. 357-359, 1977.
[48] J. Feinberg, "Optical phase conjugation in photorefractive materials," in *Optical Phase Conjugation*, R. A. Fisher, Ed. New York: Academic, 1983, pp. 435-443.
[49] J. W. Goodman, F. J. Leonberger, S. Y. Kung, and R. A. Athale, "Optical interconnections for VLSI systems," *Proc. IEEE*, vol. 72, pp. 850-866, 1984.
[50] B. Fischer, S. Weiss, and S. Sternklar, "Spatial light modulation and filtering effects in photorefractive wave mixing," *Appl. Phys. Lett.*, vol. 50, pp. 483-485, 1987.
[51] B. Fischer, S. Sternklar, and S. Weiss, "Photorefractive oscillation with intracavity image and multimode fiber," *Appl. Phys. Lett.*, vol. 48, pp. 1567-1569, 1986.
[52] J. O. White and A. Yariv, "Real-time image processing via four-wave mixing in a photorefractive medium," *Appl. Phys. Lett.*, vol. 37, pp. 5-7, 1980.
[53] B. Ya. Zeldovich, N. F. Pilipetsky, and V. V. Shkunov, *Principles of Phase Conjugation*, T. Tamir, Ed. New York: Springer, 1985, ch. 4.
[54] See, for example, A. Yariv, *Quantum Electronics*. New York: Wiley, 1975, ch. 19.
[55] B. Crosignani and A. Yariv, "Degenerate four-wave mixing in the presence of nonuniform pump wave fronts," *J. Opt. Soc. Amer. A*, vol. 1, pp. 1034-1039, 1984.
[56] B. T. Anderson, P. R. Forman, and F. C. Jahoda, "Self-pumped phase conjugation in $BaTiO_3$ at 1.06 μm," *Opt. Lett.*, vol. 10, pp. 627-629, 1985.
[57] G. Martin and R. Hellwarth, "Infrared-to-optical conversion by Bragg reflection from thermally induced index gratings," *Appl. Phys. Lett.*, vol. 34, pp. 371-373, 1979.
[58] A. M. C. Smout and R. W. Eason, "Analysis of mutually incoherent beam coupling in $BaTiO_3$," *Opt. Lett.*, vol. 12, pp. 498-500, 1987.
[59] M. D. Ewbank, "Mechanism for photorefractive phase conjugation using incoherent beams," *Opt. Lett.*, vol. 13, pp. 47-49, 1988.
[60] S. Weiss, M. Segev, S. Sternklar, and B. Fischer, "Photorefractive dynamic optical interconnects," *Appl. Opt.*, vol. 27, pp. 3422-3428, 1988.
[61] H. J. Caulfield, J. Shamir, and Q. He, "Flexible two-way optical interconnections in layered computers," *Appl. Opt.*, vol. 26, pp. 2291-2292, 1987.
[62] S. Weiss, M. Segev, and B. Fischer, "Line narrowing and self-frequency scanning of laser diode arrays coupled to a photorefractive oscillator," *IEEE J. Quantum Electron.*, vol. 24, pp. 706-708, 1988.

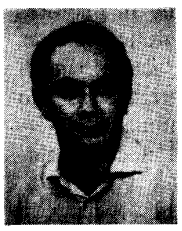

Baruch Fischer received the Ph.D. degree in physics from Bar-Ilan University, Israel, in 1980.

From 1980 to 1982 he was a Weizmann Research Fellow at the California Institute of Technology, Pasadena, and he is now an Associate Professor with the Department of Electrical Engineering in the Technion—Israel Institute of Technology, Haifa. His current research interests are in the areas of nonlinear and photorefractive optics.

Shmuel Sternklar received the B.Sc. degree in electrical engineering from the Polytechnic Institute of New York, Brooklyn, in 1980, the M.Sc. degee in bioengineering from the University of Pennsylvania, Philadelphia, in 1982, and the Ph.D. degree from the Technion—Israel Institute of Technology, Haifa, in 1987 in the field of optical processing and photorefractive materials. He is currently a Lady Davis Fellow at the Technion.

Dr. Sternklar is a member of the Optical Society of America and the SPIE.

Shimon Weiss received the B.Sc. degree in electrical engineering from the Technion–Israel Institute of Technology, Haifa, in 1984.

He is currently pursuing the Ph.D. degree. His research subject deals with wave mixing in photorefractive materials.

Mr. Weiss is a member of the Optical Society of America and the SPIE.